

CMS-HIG-21-020

CERN-EP-2024-162
2024/12/11

Measurement of boosted Higgs bosons produced via vector boson fusion or gluon fusion in the $H \rightarrow b\bar{b}$ decay mode using LHC proton-proton collision data at $\sqrt{s} = 13$ TeV

The CMS Collaboration^{*}

Abstract

A measurement is performed of Higgs bosons produced with high transverse momentum (p_T) via vector boson or gluon fusion in proton-proton collisions. The result is based on a data set with a center-of-mass energy of 13 TeV collected in 2016–2018 with the CMS detector at the LHC and corresponds to an integrated luminosity of 138 fb^{-1} . The decay of a high- p_T Higgs boson to a boosted bottom quark-antiquark pair is selected using large-radius jets and employing jet substructure and heavy-flavor taggers based on machine learning techniques. Independent regions targeting the vector boson and gluon fusion mechanisms are defined based on the topology of two quark-initiated jets with large pseudorapidity separation. The signal strengths for both processes are extracted simultaneously by performing a maximum likelihood fit to data in the large-radius jet mass distribution. The observed signal strengths relative to the standard model expectation are $4.9^{+1.9}_{-1.6}$ and $1.6^{+1.7}_{-1.5}$ for the vector boson and gluon fusion mechanisms, respectively. A differential cross section measurement is also reported in the simplified template cross section framework.

Published in the Journal of High Energy Physics as doi:10.1007/JHEP12(2024)035.

1 Introduction

The observation at the CERN LHC of a Higgs boson (H) consistent with the standard model (SM) expectation and the subsequent measurements of its properties [1–6] have advanced the understanding of electroweak (EW) symmetry breaking and the origin of the mass of fundamental particles [7–14]. Higgs boson production at high momentum transfer can be a sensitive probe of beyond the SM (BSM) physics at high energy scales, and measurements in this regime provide important input for effective field theory interpretations of H interactions [15–20]. Thus, studying Higgs bosons at high transverse momentum (p_T) has become an integral part of the physics program at the LHC.

The Higgs boson decay to a bottom quark-antiquark pair ($b\bar{b}$) has the highest branching fraction of any H decay mode in the SM [21]. When the Higgs boson is produced with high momentum, the $H \rightarrow b\bar{b}$ decay products are merged into a single large-radius jet. This distinctive boosted jet topology can be identified by its substructure and heavy flavor properties, and as a result the $H \rightarrow b\bar{b}$ decay provides an important channel for the exploration of Higgs boson production at high p_T .

Leading order (LO) Feynman diagrams of the three H production mechanisms with highest cross section in proton-proton (pp) collisions are shown in Fig. 1: gluon fusion (ggF), vector boson fusion (VBF), and vector boson associated production (VH). A small contribution to the H cross section also arises from associated production with a top quark-antiquark pair ($t\bar{t}H$). The dominant SM contribution comes from ggF, which contributes 87% of the H cross section at $\sqrt{s} = 13$ TeV when considering the full range of Higgs boson p_T . However, the relative contribution from ggF is expected to decrease with the p_T of the Higgs boson, contributing only 50 (30)% of the cumulative H cross section for $p_T > 450$ (1200) GeV [22]. While the relative contribution from VH increases as a function of Higgs boson p_T , that of VBF has minimal p_T dependence. Each of these production mechanisms provides a different probe of H interactions, and precise measurement of each one is necessary to investigate all possible manifestations of BSM physics in the Higgs sector.

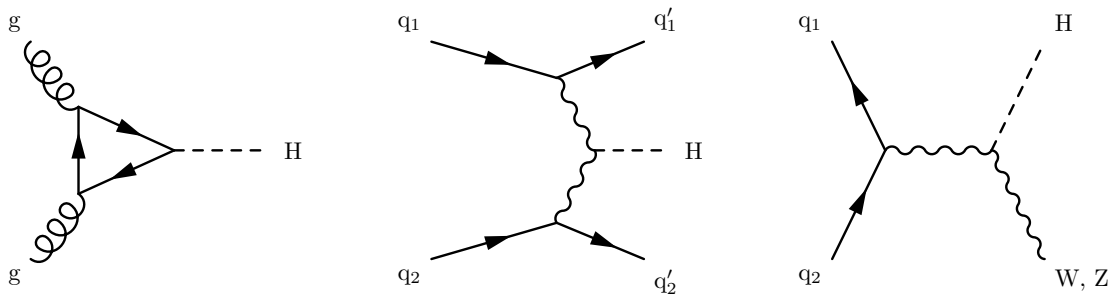


Figure 1: Lowest order Feynman diagrams of the Higgs boson production modes with highest cross section in 13 TeV proton-proton collisions, from left to right: gluon fusion, vector boson fusion, and vector boson associated production.

Existing searches in the boosted $H \rightarrow b\bar{b}$ channel from the ATLAS and CMS experiments have focused on inclusive Higgs boson production [23–25] or associated production with a vector boson [26–28]. This work extends, for the first time, high- p_T Higgs boson measurements in the $H \rightarrow b\bar{b}$ channel to VBF production. The analysis is performed using pp collision data collected with the CMS detector at the LHC in 2016–2018, corresponding to an integrated luminosity of 138 fb^{-1} [29–31]. The VBF process, which is sensitive to H couplings to vector bosons, and the ggF process, which is primarily sensitive to H couplings to top quarks and gluons, are

measured simultaneously. In order to disentangle the two processes, the analysis is performed in two categories. The first category is enriched in VBF events and targets the characteristic topology of two quark-initiated jets with high pseudorapidity (η). The second category is enriched in ggF events.

In both categories, the $H \rightarrow b\bar{b}$ decay mode is isolated from quark- and gluon-initiated jets by a multivariate large-radius jet classifier known as the DeepDoubleB (DDB) tagger [32]. Updates with respect to the previous version of the DDB tagger [33, 34] yield a gain in expected signal significance of about a factor of 2 compared to the previous CMS $H \rightarrow b\bar{b}$ search [25]. As a result, the analysis reported here provides not only the first measurement of H production via VBF at high p_T , but also the most precise measurement of ggF Higgs boson production in this regime, superseding the measurement in Ref. [25].

2 The CMS detector

The CMS apparatus [35] is a multipurpose, nearly hermetic detector, designed to trigger on [36, 37] and identify electrons, muons, photons, and hadrons [38–40]. Information about particles traversing the detector is provided by the all-silicon inner tracker, and by the crystal electromagnetic and brass-scintillator hadron calorimeters, all of which operate inside a 3.8 T superconducting solenoid, and by the gas-ionization muon detectors embedded in the flux-return yoke outside the solenoid.

Events of interest are selected using a two-tiered trigger system. The first level, composed of custom hardware processors, uses information from the calorimeters and muon detectors to select events at a rate of around 100 kHz within a fixed latency of about $4\ \mu s$ [36]. The second level, known as the high-level trigger, consists of a farm of processors running a version of the full event reconstruction software optimized for fast processing, and reduces the event rate to around 1 kHz before data storage [37].

A more detailed description of the CMS detector, together with a definition of the coordinate system used and the relevant kinematic variables, can be found in Ref. [35].

The dataset used in this analysis is divided into four data-taking periods to account for the 2017 upgrade of the CMS tracking detector, differences in accelerator and detector conditions, and updates to reconstruction algorithms and calibrations. These data-taking periods correspond to early 2016, late 2016, 2017, and 2018. Data from 2016 is split into an early and a late data-taking period due to changes made mid-year.

3 Simulated samples

Simulated samples of signal and background events are produced using various Monte Carlo (MC) event generators, with the CMS detector response modeled by GEANT4 [41]. Independent samples are generated for each of the four data-taking periods using identical generator configurations, but accounting for changes in the accelerator and detector running conditions.

The background from jets produced via the strong interaction, referred to as quantum chromodynamics (QCD) multijet events, is modeled at LO accuracy using the MADGRAPH5_aMC@NLO 2.6.5 generator [42] with up to four partons from the matrix element calculation.

The $W+jets$ and $Z+jets$ processes are modeled at LO accuracy using the MADGRAPH5_aMC@NLO generator. These samples include decays of the bosons to all flavors of quarks and up to three (four) extra partons at the matrix element level for $W+jets$ ($Z+jets$). Jets from the matrix ele-

ment calculations and parton shower description are matched using the MLM prescription [43]. Correction factors are applied to the $W+jets$ and $Z+jets$ samples to match the generator-level p_T distributions with those predicted by the highest available order in the perturbative expansion. The QCD next-to-LO (NLO) corrections are derived using MADGRAPH5_aMC@NLO, simulating W and Z boson production with up to two additional partons and FxFx matching to the parton shower [44]. The EW NLO corrections are taken from theoretical calculations in Refs. [45–48].

Electroweak production of W and Z bosons is modeled using MADGRAPH5_aMC@NLO at LO accuracy. Diboson processes are modeled at LO accuracy with PYTHIA 8.226 [49], and the total cross sections are corrected to next-to-NLO (NNLO) accuracy with the MCFM 7.0 program [50]. Top quark-antiquark ($t\bar{t}$) and single top quark production are modeled at NLO in QCD using POWHEG 2.0 [51–55].

The ggF Higgs boson production process is simulated using the HJMINLO event generator [56, 57] with the Higgs boson mass set to 125 GeV. Finite top quark mass effects [58] are included following the recommendation in Ref. [22]. The POWHEG generator [59–61] is used to model Higgs boson production via VBF, VH, and $t\bar{t}H$ at NLO accuracy. The VBF sample is reweighted to account for NNLO corrections to the p_T spectrum and N^3LO corrections to the inclusive cross section [62, 63]. These corrections have a negligible effect on the yield for this process for events with Higgs boson $p_T > 450$ GeV. EW corrections are also applied to the VBF, VH, and $t\bar{t}H$ processes [22].

For parton showering and hadronization, all generated samples are interfaced with PYTHIA 8.230, with the parameters for the underlying event description set via the CP5 tune [64]. The diboson process exceptionally uses PYTHIA 8.226 for both the matrix element and parton shower evolution. The parton distribution function (PDF) set NNPDF3.1 [65] at NNLO accuracy is used for all processes.

4 Event reconstruction and selection

The particle-flow (PF) algorithm [66] aims to reconstruct and identify each individual particle in an event using an optimized combination of information from the various elements of the CMS detector. The primary vertex is taken to be the vertex corresponding to the hardest scattering in the event, evaluated using tracking information alone, as described in Ref. [40].

Jets are reconstructed by clustering PF candidates using the anti- k_T algorithm [67] as implemented in the FASTJET software package [68]. Small-radius jets are clustered with a distance parameter of 0.4. Large-radius jets, which are used to capture the decay products of heavy boosted objects, use a distance parameter of 0.8 [69].

Jet momentum is taken to be the vectorial sum of all PF candidate momenta in the jet. Additional pp interactions within the same or nearby bunch crossings, known as pileup, can increase the apparent jet momentum by contributing additional tracks and calorimetric energy deposits. To mitigate this effect for small-radius jets, tracks originating from pileup vertices are discarded and an offset correction is applied to correct for remaining contributions [70]. For large-radius jets, the pileup per particle identification algorithm [71] is used to weight the PF candidates prior to jet clustering. Jet energy corrections are derived from simulation to bring the measured response of jets to that of particle level jets on average [72]. Additional selection criteria are applied to remove jets that are likely to be dominated by instrumental effects or reconstruction failures [69, 70].

To isolate the H signal, a large-radius jet with high p_T is required. Events are selected by a combination of triggers, with each trigger imposing a minimum threshold on either the p_T of a large-radius jet or the event H_T , the scalar p_T sum of all small-radius jets in the event with $|\eta| < 3$. For large-radius jets used in the trigger selection, a minimum trimmed jet mass [73] is also required. The trigger selection is about 90% efficient with respect to the offline selection for events containing large-radius jets with p_T from 450–500 GeV and $|\eta| < 2.5$, and is fully efficient for $p_T > 500$ GeV and $|\eta| < 2.5$. In order to ensure high trigger efficiency, each event is required to contain at least one large-radius jet with $p_T > 450$ GeV and $|\eta| < 2.5$. Large-radius jets are required to pass the tight jet identification requirement [69] and be separated from all isolated photons or charged leptons by a distance of $\Delta R = \sqrt{\Delta\eta^2 + \Delta\phi^2} > 0.8$, where $\Delta\eta$ and $\Delta\phi$ are the differences in pseudorapidity and azimuthal angle, respectively.

For large-radius jets originating from the decay of a massive boson (W, Z, H), contamination from underlying event and pileup can lead to an overestimate of the jet invariant mass and degraded jet mass resolution. The soft drop algorithm [74], with parameters $\beta = 0$ and $z_{\text{cut}} = 0.1$, is applied to mitigate these effects by removing PF candidates consistent with soft and wide-angle radiation from the jet. For jets originating from the decay of a massive boson, the soft drop mass (m_{SD}) peaks at the boson mass, while for quark- and gluon-initiated jets, m_{SD} has a smoothly falling spectrum.

In order to avoid regions where non-perturbative effects lead to discrepancies in generator predictions [75], large-radius jets are required to have $\rho > -6.0$, where $\rho = 2 \ln(m_{\text{SD}}/p_T)$. Large-radius jets with $\rho > -2.1$ are also vetoed, since above this threshold the jet constituents are no longer fully contained in a cone of $R = 0.8$. This ρ selection is fully efficient for H signal events.

The multivariate DDB tagger discriminant is used to determine whether a large-radius jet originates from a heavy particle decaying to a $b\bar{b}$ pair [32]. The DDB tagger is based on a deep neural network that is trained to distinguish large-radius jets containing scalar $X \rightarrow b\bar{b}$ decays from jets originating from light quarks or gluons. The DDB tagger is trained on jet features, such as the number of PF candidates and low-level quantities describing secondary vertices within the jet. The addition of low-level features leads to a large improvement in performance relative to the previous version of the tagger [33, 34]: for a QCD jet mistag rate of 1%, the signal efficiency of the updated DDB tagger is about 75%, representing an improvement of about 50% with respect to the previous version.

In order to ensure that the DDB tagger selection does not impact the shape of the background m_{SD} distribution, the DDB network is trained on a signal sample composed of simulated decays of bosons with masses ranging from 20 to 200 GeV. The success of this decorrelation method is demonstrated in Fig. 2, which shows the shape of the m_{SD} distribution for simulated QCD jets with $450 < p_T < 1200$ GeV after different DDB selection criteria have been applied. The shape of the m_{SD} distribution is shown to be mostly independent of the DDB threshold value.

The large-radius jet with the highest DDB score is identified as the Higgs boson candidate. This criterion selects a H candidate jet within $\Delta R < 0.8$ of the generated particle in more than 90% of simulated $H \rightarrow b\bar{b}$ events. Events in which the selected candidate jet does not correspond to the H decay are excluded from the signal yield, and their contribution is accounted for in the estimation of the QCD multijet background.

Events containing H candidate jets with high DDB tagger score enter the “DDB pass” region. The definition of the DDB pass region is chosen to maximize the expected sensitivity to VBF H production, and the DDB tagger threshold corresponds to a signal efficiency of about 40%

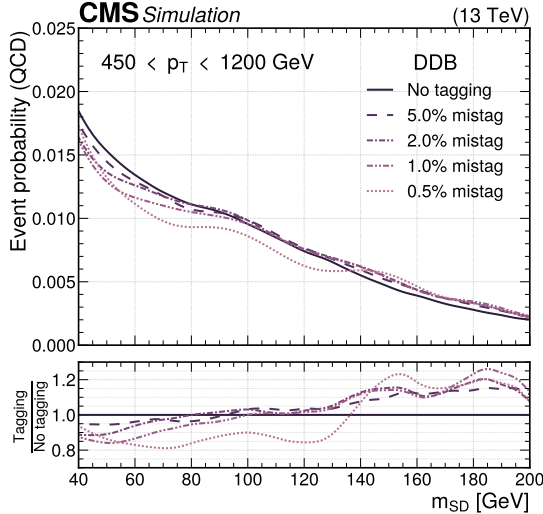


Figure 2: Soft drop mass distribution in simulated QCD events after applying the DDB selection at different working points. The distributions are obtained from simulated QCD events, smoothed using Gaussian kernel density estimation, and normalized to unit area. The lower panel shows the ratio to the inclusive distribution.

and a QCD multijet mistag rate of 0.5%. Events containing H candidate jets below this DDB threshold enter the “DDB fail” region, which is later used to constrain the normalization and shape of the QCD multijet background.

Higgs boson candidate jets are required to be consistent with the two-prong substructure of a $H \rightarrow b\bar{b}$ decay, reducing the contribution from $t\bar{t}$, single top, and QCD backgrounds. The substructure selection is based on the N_2^1 variable, a ratio of three-point to two-point energy correlation functions proposed in Ref. [76]. In order to minimize the dependence of the substructure selection on the p_T and m_{SD} of the H candidate, a variant of N_2^1 is defined using the designed decorrelated tagger (DDT) technique [77]. The value of N_2^1 that results in a background efficiency ϵ is determined as a function of jet p_T and ρ and denoted $N_\epsilon(p_T, \rho)$. A decorrelated substructure variable, which has a background efficiency that is independent of jet p_T and ρ , can be obtained by subtracting $N_\epsilon(p_T, \rho)$ from the nominal substructure variable. The following transformation defines the decorrelated substructure variable used in this analysis:

$$N_2^{1,DDT} = N_2^1 - N_\epsilon(p_T, \rho). \quad (1)$$

A background efficiency of $\epsilon = 0.26$ is chosen to maximize the total H signal sensitivity, and $N_{0.26}(p_T, \rho)$ is derived from the simulated multijet distribution of N_2^1 separately in each data-taking period. Selected events are required to have $N_2^{1,DDT} < 0$, which retains about 50% of H signal events and (by construction) rejects 74% of expected QCD events. The calibration of this substructure requirement and the associated uncertainties are described in Section 5.2.

Small-radius jets are required to have $p_T > 30$ GeV and $|\eta| < 5.0$. These jets must be separated from the H candidate jet by a distance of $\Delta R > 0.8$. The DEEPJET algorithm [78, 79] is used to identify small-radius jets within the volume of the silicon tracking detectors ($|\eta| < 2.5$) that originate from b quarks. In order to reduce contamination from $t\bar{t}$ background, events are vetoed if any of the four highest- p_T small-radius jets in the hemisphere opposite the H candidate is b tagged.

The missing transverse momentum vector \vec{p}_T^{miss} is computed as the negative vector sum of the transverse momenta of all the PF candidates in an event, with modifications to account for

corrections to the energy scale of the reconstructed jets in the event [80]. The magnitude of \vec{p}_T^{miss} is denoted p_T^{miss} and required to be less than 140 GeV.

Events containing charged leptons are vetoed. For purposes of this veto, electrons must have $p_T > 10 \text{ GeV}$ and $|\eta| < 2.5$ and pass the loose identification criteria outlined in Ref. [38]. Muons must satisfy the loose identification criteria described in Ref. [39] and have $p_T > 10 \text{ GeV}$ and $|\eta| < 2.4$. For electrons (muons), the isolation variable corresponds to the pileup-corrected sum p_T of charged hadrons and neutral particles in a cone of $R = 0.3$ (0.4) around the lepton divided by the lepton p_T . The isolation is required to be less than 0.15 and 0.25 for electrons and muons, respectively. Hadronically decaying tau leptons (τ_h) are reconstructed from jets using the hadrons-plus-strips algorithm [81]. To distinguish genuine τ_h decays from jets originating from the hadronization of quarks or gluons, as well as from electrons or muons, the DEEPTAU algorithm is used [82]. For the purposes of a lepton veto, τ_h must have $p_T > 20 \text{ GeV}$ and $|\eta| < 2.3$.

In order to measure the VBF and ggF production mechanisms simultaneously, the selected events (both DDB pass and fail) are partitioned into two categories. The VBF category selection is optimized for sensitivity to VBF production by targeting the characteristic forward (high $|\eta|$) quark-initiated jets. Events entering this category are required to contain two small-radius jets in addition to the H candidate. The small-radius jets are required to have a pseudorapidity separation of $|\Delta\eta| > 3.5$ and invariant mass of $m_{jj} > 1 \text{ TeV}$, where the selection criteria are chosen to maximize the sensitivity to VBF production. If an event contains more than two small-radius jets, the highest and second highest in p_T are used to construct $\Delta\eta$ and m_{jj} . Events containing fewer than two small-radius jets, or where $|\Delta\eta| < 3.5$ or $m_{jj} < 1 \text{ TeV}$, fall into the ggF category. Figure 3 shows the predicted relative contribution of each production mechanism to the total Higgs boson signal in the VBF and ggF categories.

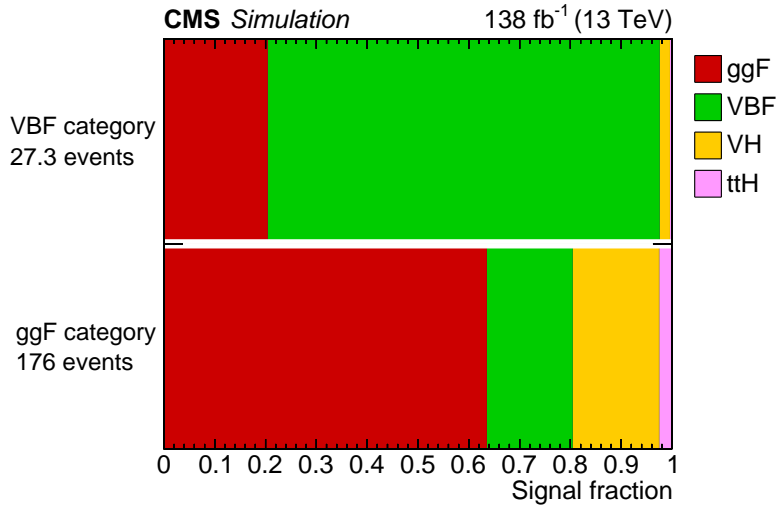


Figure 3: Simulated relative contributions of the four leading H production processes to the total H signal yield in the VBF and ggF categories, shown in the DDB pass region. Small contributions from the VH and $t\bar{t}H$ processes are also included. The total number of predicted H events in the 138 fb^{-1} dataset are 27.3 and 176 in the VBF and ggF categories, respectively.

The VBF category is divided into two bins in m_{jj} with different signal purity: $1 < m_{jj} < 2 \text{ TeV}$ and $m_{jj} > 2 \text{ TeV}$. When combined statistically, this yields about 20% improvement in the expected significance of a VBF signal compared to a single bin. Similarly, the ggF category is divided into six bins in the H candidate jet p_T with boundaries 450, 500, 550, 600, 675, 800,

and 1200 GeV. The upper p_T bound of 1200 GeV does not have a significant impact on the sensitivity and excludes a region where the QCD multijet background is difficult to model. The subdivision into p_T bins improves the expected ggF significance by about 20%.

5 Background estimation

Because of its large cross section, QCD multijet production is the dominant background in the combined DDB pass and fail regions. Significant resonant backgrounds arise from W+jets and Z+jets processes, where the two-prong decay of a high- p_T vector boson is mistagged as a H candidate. Electroweak W and Z boson production contribute in particular to the background in the VBF category because of the presence of two forward quark-initiated jets. For events in which a high- p_T top quark is produced, it is possible that a large-radius jet captures only two of the three prongs of the decay and passes the $N_2^{1,\text{DDT}}$ selection. The presence of a bottom quark in these decays makes them more likely to pass the DDB requirement. In this way, top quark production contributes to the nonresonant component of the background. This section describes the estimate of the background contribution from each of these processes.

Additional small background contributions from diboson, VH, and $t\bar{t}H$ processes (each expected to be < 1% of the total background) are estimated from simulation. Both VH and $t\bar{t}H$ are assumed to occur at SM rates.

5.1 QCD background

The soft drop jet mass in QCD multijet events follows a steeply falling distribution. The predicted shape of the QCD background in the DDB pass region is derived using data in the background-enriched DDB fail region. The full prediction of the QCD background yield in the DDB pass region takes the form

$$N_P^i = N_F^{\text{data},i} R_{P/F}^{\text{MC},i} T_{P/F}(p_T^i, \rho^i) T_{\text{res}}(p_T^i, \rho^i), \quad (2)$$

where bin i corresponds to p_T^i and ρ^i . $N_F^{\text{data},i}$ is the number of data events minus the number of predicted non-QCD background events in bin i in the DDB fail region. The ratio $R_{P/F}^{\text{MC},i}$ is the number of simulated QCD events in the DDB pass region divided by that in the DDB fail region.

Two transfer factors, $T_{P/F}$ and T_{res} , account for shape differences in the jet p_T and m_{SD} distributions between the DDB pass and fail regions. In the ggF category, the functional form of each transfer factor is taken to be a two-dimensional Bernstein polynomial in the H candidate jet p_T and ρ :

$$T_{P/F}(p_T, \rho) = \sum_{k=0}^{n_\rho} \sum_{l=0}^{n_{p_T}} a_{k,l} [b_{k,n_\rho}(\rho) b_{l,n_{p_T}}(p_T)], \quad (3)$$

where n_ρ and n_{p_T} are the degrees of the polynomial in ρ and p_T , respectively, $a_{k,l}$ are fitted coefficients, and $b_{v,n}$ are one-dimensional Bernstein polynomials:

$$b_{v,n}(x) = \binom{n}{v} x^v (1-x)^{n-v}. \quad (4)$$

The variables p_T and ρ are affine transformed to lie within the domain of the Bernstein basis. Because the VBF category is not binned in p_T , the transfer factors in this category are parameterized only in ρ , and a sum of one-dimensional Bernstein polynomials is used.

The first transfer factor, $T_{\text{P/F}}$, accounts for possible p_{T} - or m_{SD} -dependent effects due to the DDB selection by parameterizing the ratio of the QCD event yield in the DDB pass and fail regions. The coefficients $a_{k,l}$ of $T_{\text{P/F}}$ are derived with a dedicated fit to the m_{SD} distribution in QCD MC simulation. Discrepancies in the tagger performance between data and simulation are accounted for with a second transfer factor, T_{res} . The coefficients of T_{res} are obtained in the final simultaneous fit to data described in Section 7. Independent transfer factors $T_{\text{P/F}}$ and T_{res} are defined for each data-taking period, and in the ggF category and each of the two m_{jj} bins in the VBF category.

For each transfer factor, the optimal number of free parameters is determined by a Fisher F-test [83]. As a first step, a low-order polynomial of n_1 parameters is taken as the baseline function. An alternative function with $n_2 > n_1$ parameters is tested against the baseline. In the case where the baseline function has $n_{\rho} = n_{p_{\text{T}}}$, the alternative function is determined by increasing the polynomial order in ρ . The alternative function is adopted as the new baseline if it provides a significantly better goodness-of-fit (F-statistic with p -value [84] less than 0.05). The polynomial order is optimized independently for $T_{\text{P/F}}$ and T_{res} , separately in each data-taking period and in the ggF category and each of the two m_{jj} bins in the VBF category.

In the ggF category, the optimal polynomial order for $T_{\text{P/F}}$ is determined to be $(n_{p_{\text{T}}}, n_{\rho}) = (1, 1)$ for early 2016 and $(n_{p_{\text{T}}}, n_{\rho}) = (0, 1)$ for late 2016, 2017, and 2018. The optimal polynomial order for T_{res} is found to be $(n_{p_{\text{T}}}, n_{\rho}) = (0, 2)$ for all data-taking periods. In the VBF category, the optimal polynomial order for both transfer factors is found to be $n_{\rho} = 0$ for all data-taking periods in both m_{jj} bins.

Tests with alternative functional forms for the transfer factors show that the final result has negligibly small dependence on the choice of the parameterization.

5.2 W+jets and Z+jets backgrounds

The W+jets and Z+jets backgrounds are modeled using simulation, with normalizations and kinematic distributions corrected for NLO QCD and EW effects, as described in Section 3. A scale factor (f_{sub}) is applied to the W+jets and Z+jets processes to correct for the efficiency of the two-prong substructure selection ($N_2^{1,\text{DDT}} < 0$). A dedicated W tag control region (CR) is used to simultaneously derive f_{sub} , a correction factor on the jet mass resolution (f_{σ}), and a jet mass shift (δ_m). These corrections are applied to the predictions from simulation for W+jets and Z+jets, as well as all H signal processes.

Events entering the W tag CR must pass a trigger requiring a muon with $p_{\text{T}} > 50 \text{ GeV}$. Events must contain a muon passing the tight identification requirements defined in Ref. [39] and have $p_{\text{T}}^{\text{miss}} > 40 \text{ GeV}$. The p_{T} of the muon plus $p_{\text{T}}^{\text{miss}}$ system, which forms a W boson proxy, must be greater than 200 GeV . Finally, at least one b-tagged small-radius jet is required. This region contains a high fraction of $t\bar{t}$ events, and the substructure variable requirements select primarily top quark decays to boosted W bosons.

Two template m_{SD} distributions are constructed from simulation in the W tag CR: events that contain a W boson, and events that do not. Variations in the jet mass scale and jet mass resolution are calculated for the template containing a W boson using linear morphing [85]. The desired corrections are then extracted from a template fit to data in the W tag CR. This fit is performed simultaneously in the regions passing and failing the two-prong substructure selection ($N_2^{1,\text{DDT}} < 0$ and $N_2^{1,\text{DDT}} > 0$, respectively).

The fitted values of f_{sub} , f_{σ} , and δ_m are shown in Table 1 with their uncertainties. These corrections are measured independently for each data-taking period in order to account for the

2017 upgrade of the CMS tracking detector, differences in pileup and detector conditions, and updates to reconstruction algorithms and calibrations. In the fit to the signal regions in data, the uncertainties on these corrections are treated as systematic uncertainties.

Table 1: Summary of corrections for the jet substructure selection (scale factor f_{sub}), jet mass resolution (scale factor f_σ), and jet mass scale (shift δ_m) for different data-taking periods.

	f_{sub}	f_σ	δ_m [MeV]
Early 2016	0.99 ± 0.16	1.13 ± 0.04	-240 ± 410
Late 2016	0.82 ± 0.15	1.21 ± 0.03	$+440 \pm 340$
2017	1.05 ± 0.10	1.09 ± 0.02	$+470 \pm 180$
2018	0.94 ± 0.08	1.07 ± 0.03	-990 ± 250

A nonresonant background arises from W+jets and Z+jets events in which the selected candidate jet does not correspond to the decay of the vector boson. Since such jets originate instead from QCD processes, they are accounted for in the QCD background estimation.

5.3 Top quark background

Top quark processes contribute a nonresonant component of a few percent to the total background. While the shape of the m_{SD} distributions in $t\bar{t}$ and single top quark processes are estimated from simulation, both the overall normalization and the DDB tagger efficiency are constrained using data. This is accomplished by including a single-muon CR, which closely mimics the signal selection described above, but selects a semileptonic decay of the $t\bar{t}$ pair rather than all-hadronic.

Events entering the single-muon CR must pass a trigger requiring a muon with $p_T > 50$ GeV. Following trigger selection, events must contain a muon with $p_T > 55$ GeV and $|\eta| < 2.1$. The muon must satisfy the loose identification requirements defined in Ref. [39] and have isolation variable less than 0.25. Events containing electrons or τ_h are vetoed. At least one large-radius jet with $p_T > 400$ GeV, $|\eta| < 2.5$, $m_{\text{SD}} > 40$ GeV and $N_2^{\text{1,DDT}} < 0$ is required, and this jet must be separated from the muon by an angular distance of $\Delta\phi > 2\pi/3$. At least one small-radius b-tagged jet with $p_T > 50$ GeV and $|\eta| < 2.5$ is also required. The resulting CR is more than 80% pure in top quark processes. Small contributions from QCD, W+jets, and Z+jets processes are estimated from simulation.

In order to account for kinematic differences between the single-muon CR and the VBF-specific phase space, an additional systematic uncertainty is applied to the $t\bar{t}$ yield in the VBF category. The magnitude of this uncertainty is derived from a comparison of the data-to-simulation scale factor obtained in the inclusive single-muon CR and in the same CR with additional requirements on the number of small-radius jets, $\Delta\eta$, and m_{jj} .

The DDB pass and fail regions of the single-muon CR are treated as single-bin counting experiments in the final fit framework.

6 Systematic uncertainties

Several sources of experimental uncertainty arise from the reconstruction and calibration of physics objects from low-level detector responses.

A data-to-simulation scale factor is applied to the $H \rightarrow b\bar{b}$ and $Z \rightarrow b\bar{b}$ predictions to account for the difference in efficiency of the DDB tagger selection. This scale factor is included in

the signal extraction fit as a constrained nuisance parameter with a nominal value of unity and a conservative uncertainty of 30%. The magnitude of this uncertainty is based on the results of dedicated measurements in QCD multijet events with gluon to $b\bar{b}$ splitting topologies similar to the $H \rightarrow b\bar{b}$ signal [86], but a precise scale factor cannot be derived due to the limited number of gluon splitting events in the p_T regime relevant for this analysis. The DDB scale factor is instead constrained *in situ* via the observed $Z \rightarrow b\bar{b}$ yield in the DDB pass and fail regions and constitutes the dominant experimental uncertainty. The extracted DDB scale factors and uncertainties are shown in Table 2.

Table 2: Post-fit DDB tagger selection efficiency scale factor and uncertainty for different data-taking periods.

	Scale factor	Uncertainty	
Early 2016	0.88	+0.19	-0.15
Late 2016	0.92	+0.18	-0.13
2017	0.79	+0.12	-0.10
2018	0.85	+0.11	-0.10

The uncertainties on the corrections for substructure selection, jet mass scale, and jet mass resolution detailed in Section 5.2 are treated as constrained nuisance parameters. These uncertainties are correlated among the W , Z , and Higgs boson production processes, and are further constrained by the presence of W and Z boson resonances in the m_{SD} distribution. Additional systematic uncertainties are applied to the event yields of W +jets, Z +jets, $t\bar{t}$, and Higgs boson production to account for the uncertainties due to the jet energy scale and resolution [72, 87] and the limited event count of simulated samples. A bin-by-bin uncertainty is applied to account for the limited number of simulated QCD events in the dedicated fit to determine the transfer factor $T_{P/F}$.

Other experimental uncertainties, including those related to the determination of the integrated luminosity [29–31], variations in the amount of pileup obtained by adjusting the total inelastic cross section, modeling of the trigger efficiency, and the isolation and identification of the veto leptons are also considered, and contribute only a few percent to the total uncertainty.

In addition to experimental uncertainties, theoretical uncertainties are included in the final fit to account for inaccuracy in the modeling of SM processes.

The dominant theoretical uncertainty is due to the renormalization and factorization scales chosen for the simulated H samples. These uncertainties are applied to all H production processes and are propagated to the total expected yield of the H signal according to the prescription recommended in Ref. [22]. They amount to approximately 20% and 5% in the ggF and VBF signal yields, respectively. Uncertainties in the event yields due to initial- and final-state radiation are also calculated for all H production processes by varying the renormalization scale and non-singular term using the PYTHIA 8 showering algorithm [88]. The Hessian PDF uncertainty is also applied to H signal yield, according to the prescription of Ref. [89].

Theoretical uncertainties on the W +jets and Z +jets processes account for missing higher-order QCD and mixed QCD-EW effects beyond the corrections described in Section 3, following the prescription of Ref. [48].

All theoretical uncertainties are considered to be correlated across all data-taking periods, and experimental systematic uncertainties are considered to be uncorrelated, with the exception of a correlated component of the uncertainty on the integrated luminosity (\mathcal{L}). All systematic uncertainties are incorporated into the analysis via nuisance parameters and treated according

to the frequentist paradigm [90].

Among the largest sources of systematic uncertainty are the theoretical uncertainties in the Higgs boson production cross section, the size of simulated signal samples, and the uncertainty in the data-to-simulation scale factor on the DDB tagger selection. Overall, the measurement is limited by the statistical uncertainty in data, including the limited sample size available to determine the QCD background yield under the Higgs boson peak via the transfer factor T_{res} , as discussed in Section 5.1.

7 Results

A binned maximum likelihood fit to the observed m_{SD} distributions is performed using the sum of the signal and background contributions. The test statistic chosen to determine the signal yield is based on the profile likelihood ratio [90]. The fit is performed simultaneously in many bins: in both m_{jj} bins of the VBF category and all p_T bins of ggF category, in the single-muon control region, in both the DDB pass and fail regions, and in all four data-taking periods. The observed data and post-fit m_{SD} distributions in the VBF category are shown in Fig. 4. For display purposes, the data and fitted distributions are summed over both m_{jj} bins and all four data-taking periods. For the ggF category, the observed data and post-fit m_{SD} distributions are shown in Fig. 5, again summed over all six p_T bins and all data-taking periods for display purposes.

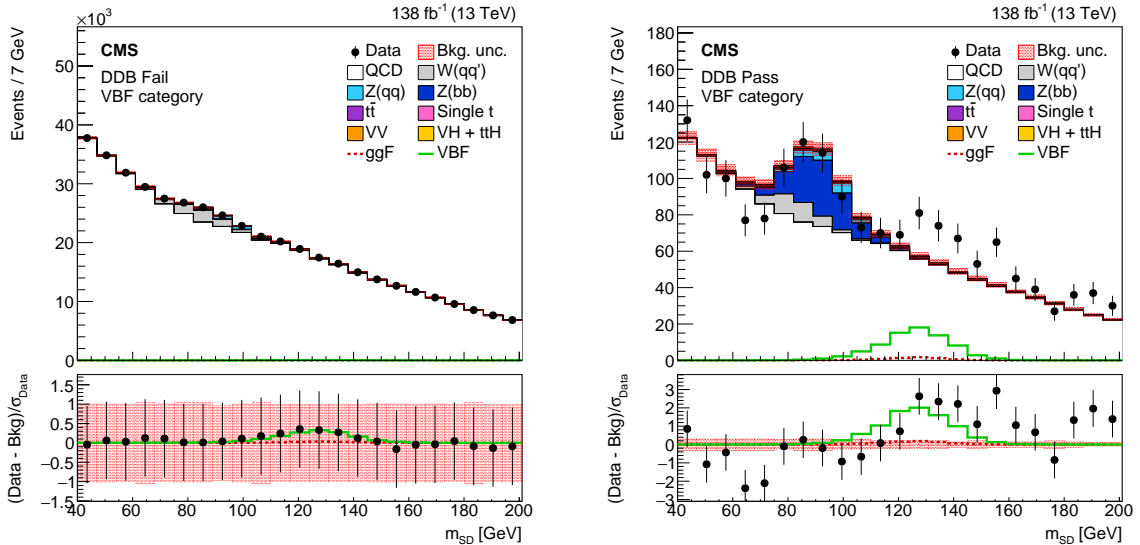


Figure 4: Post-fit soft drop mass distribution in the VBF category, summed over all m_{jj} bins and data-taking periods for display purposes. The DDB fail (left) and pass (right) regions are shown. The total background is broken down into contributions from different processes, and the total uncertainty is shown as a red band. The lower panels show the difference between the data and background prediction divided by the statistical uncertainty in data. The near-perfect model agreement with data in the DDB fail region is by construction. The ggF and VBF distributions are overlaid in red and green, respectively. Each signal is scaled to its fitted event yield.

The best fit value of the signal strength, defined as the ratio of the measured to the SM expected cross section times $H \rightarrow bb$ branching fraction, and an approximate 68% confidence level (CL) interval are extracted following Ref. [91]. The fitted signal strengths for VBF and ggF

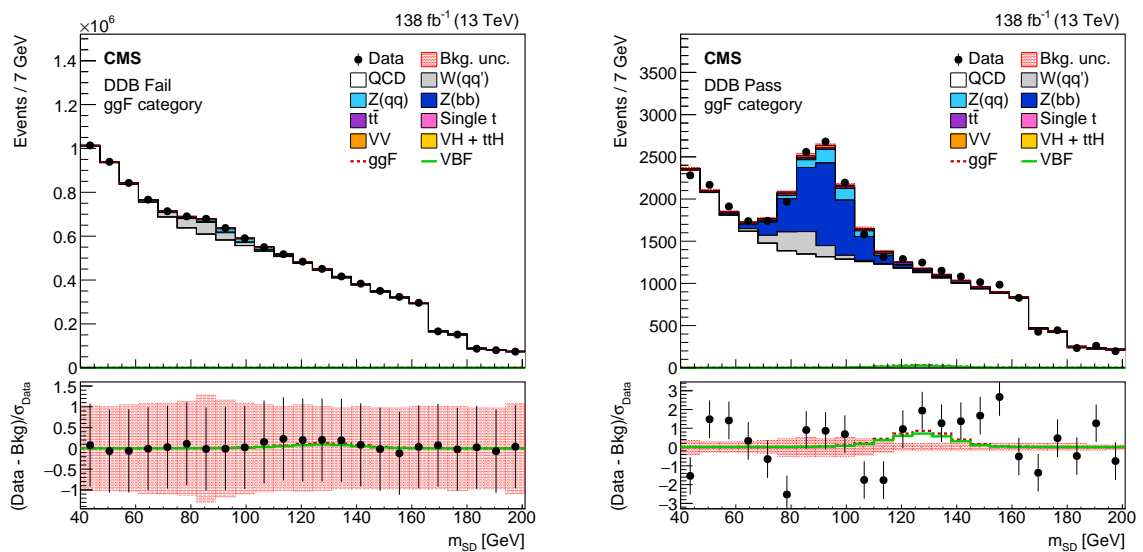


Figure 5: Post-fit soft drop mass distribution in the ggF category, summed over all p_T bins and data-taking periods for display purposes. The DDB fail (left) and pass (right) regions are shown. The total background is broken down into contributions from different processes, and the total uncertainty is shown as a red band. The lower panels show the difference between the data and background prediction divided by the statistical uncertainty in data. The near-perfect model agreement with data in the DDB fail region is by construction. The ggF and VBF distributions are overlaid in red and green, respectively. Each signal is scaled to its fitted event yield. The apparent discontinuity at high mass is due to the exclusion of bins with extreme values of ρ .

Table 3: Fitted signal strength for $H \rightarrow b\bar{b}$ in the VBF and ggF channels for each data-taking period and for the full data set. The total uncertainty is shown, followed by the statistical component in parentheses.

	$\mathcal{L} [\text{fb}^{-1}]$	VBF signal strength	ggF signal strength
Early 2016	19.5	$5.2^{+4.6}_{-3.8} (+3.9 \text{ stat})$	$2.5^{+4.7}_{-4.3} (+3.8 \text{ stat})$
Late 2016	16.8	$5.6^{+5.8}_{-4.2} (+4.5 \text{ stat})$	$0.6^{+4.4}_{-4.8} (\pm 3.8 \text{ stat})$
2017	41.5	$0.8^{+2.8}_{-2.5} (+2.7 \text{ stat})$	$3.3^{+3.1}_{-2.7} (\pm 2.5 \text{ stat})$
2018	59.8	$8.3^{+3.9}_{-3.0} (+2.8 \text{ stat})$	$0.4^{+2.6}_{-2.7} (\pm 2.3 \text{ stat})$
Combined	138	$4.9^{+1.9}_{-1.6} (\pm 1.5 \text{ stat})$	$1.6^{+1.7}_{-1.5} (\pm 1.4 \text{ stat})$

H production, denoted μ_{VBF} and μ_{ggF} , respectively, are extracted separately for the four data-taking periods, and a combined fit over the full data set is performed for the final result. The VH and $t\bar{t}H$ processes are assumed to occur at SM rates. The results are summarized in Table 3. The combined signal strength for the VBF process is measured to be $4.9^{+1.9}_{-1.6}$, and the combined signal strength for the ggF process is measured to be $1.6^{+1.7}_{-1.5}$. The expected signal strengths for VBF and ggF are $1.0^{+1.4}_{-1.3}$ and $1.0^{+1.4}_{-1.3}$, respectively. The observed (expected) correlation between these two signal strengths is -0.41 (-0.41). Tabulated results are provided in the HEPData record for this analysis [92].

Figure 6 shows the combined two-dimensional likelihood scan performed over the VBF and ggF signal strengths. The best fit point differs from the SM expectation by 2.7σ , and from the null hypothesis (no H production) by 4.0σ .

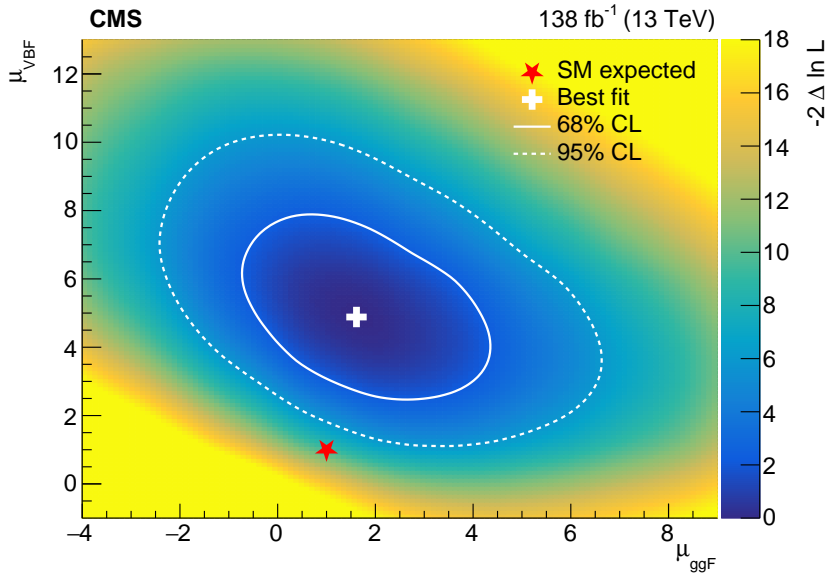


Figure 6: Two-dimensional likelihood contour of the VBF and ggF signal strengths. The color scale represents twice the negative log likelihood difference with respect to the best fit point. The observed 95% (dashed) and 68% (solid) contours are shown in white, and the best fit point as a white cross. The SM expectation is marked by a red star.

7.1 Differential measurement

The observed m_{SD} distributions in the DDB pass region are shown separately in each bin in Figs. 7 and 8, for VBF and ggF, respectively. The signal strength is also fitted independently per reconstruction-level bin. Because the VBF (ggF) category can only weakly constrain the ggF (VBF) process, the ratio of ggF to VBF is fixed to the value obtained in the signal strength fit described above. The results are shown in Fig. 9.

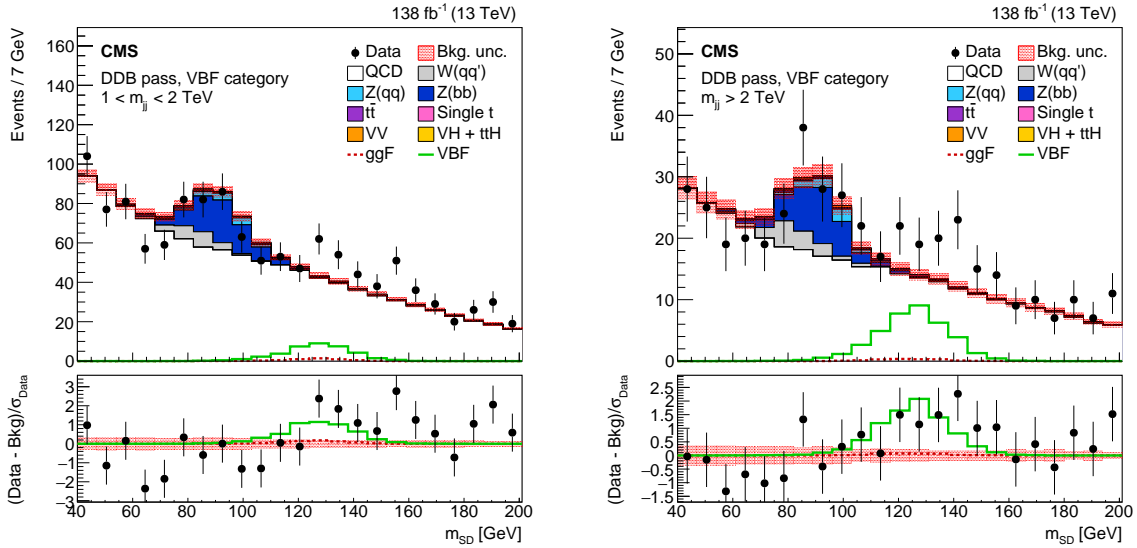


Figure 7: Post-fit soft drop mass distribution in each of the two m_{jj} bins in the VBF category, summed over all data-taking periods for display purposes. The DDB pass region is shown. The lower panels show the difference between the data and background prediction divided by the statistical uncertainty in data. The ggF and VBF distributions are overlaid in red and green, respectively. Each signal is scaled to its fitted event yield.

A maximum likelihood unfolding technique [93] is used to remove the effects of limited detector acceptance and response on the measured production cross section. The fiducial cross section is extracted simultaneously in five bins, each of which is considered as a separate process and modified by a freely floating signal strength parameter in the likelihood model. The three bins in the ggF channel correspond to fiducial regions with generated Higgs boson rapidity $|y^{H,\text{gen}}| < 2.5$ and $p_T(p_T^{H,\text{gen}})$ in the ranges 300–450, 450–650, and $> 650 \text{ GeV}$. The two bins in the VBF channel correspond to rapidity $|y^{H,\text{gen}}| < 2.5$, $p_T^{H,\text{gen}} > 200 \text{ GeV}$, and m_{jj}^{gen} in the ranges 1000–1500 GeV and $> 1500 \text{ GeV}$, where m_{jj}^{gen} is the generator-level invariant mass of the forward quark-initiated jets. This choice of bins is consistent with the simplified template cross section (STXS) stage 1.2 scheme [21, 94]. Additional STXS bins corresponding to ggF with $p_T^{H,\text{gen}} < 300 \text{ GeV}$ and VBF with $p_T^{H,\text{gen}} < 200 \text{ GeV}$ or $m_{jj}^{\text{gen}} < 1000 \text{ GeV}$ are found to have negligible contribution to the signal region. The H signal yields in these bins are assumed to occur at SM rates.

For the theoretical uncertainties, only those that affect the acceptance of signal events in the analysis selection are taken into account. Each fitted signal strength parameter and its uncertainty are scaled by the corresponding simulated cross section to obtain the best fit estimator for the cross section and its uncertainty.

The unfolded fiducial cross sections are shown in Fig. 10, with the predictions from the signal event generators overlaid. The measured cross sections and uncertainties are also reported in

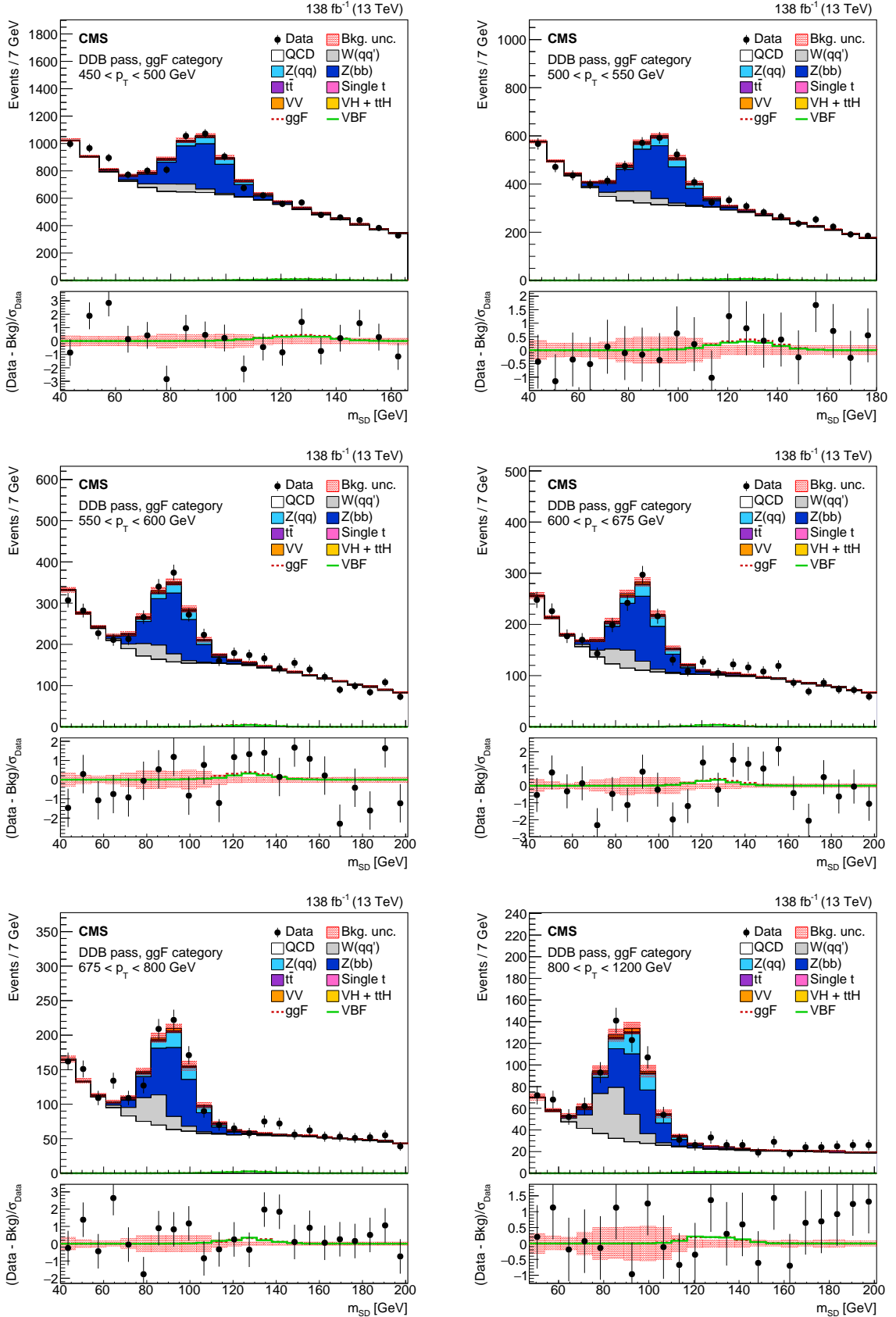


Figure 8: Post-fit soft drop mass distribution in each of the p_T bins in the ggF category, summed over all data-taking periods for display purposes. The DDB pass region is shown. The lower panels show the difference between the data and background prediction divided by the statistical uncertainty in data. The ggF and VBF distributions are overlaid in red and green, respectively. Each signal is scaled to its fitted event yield.

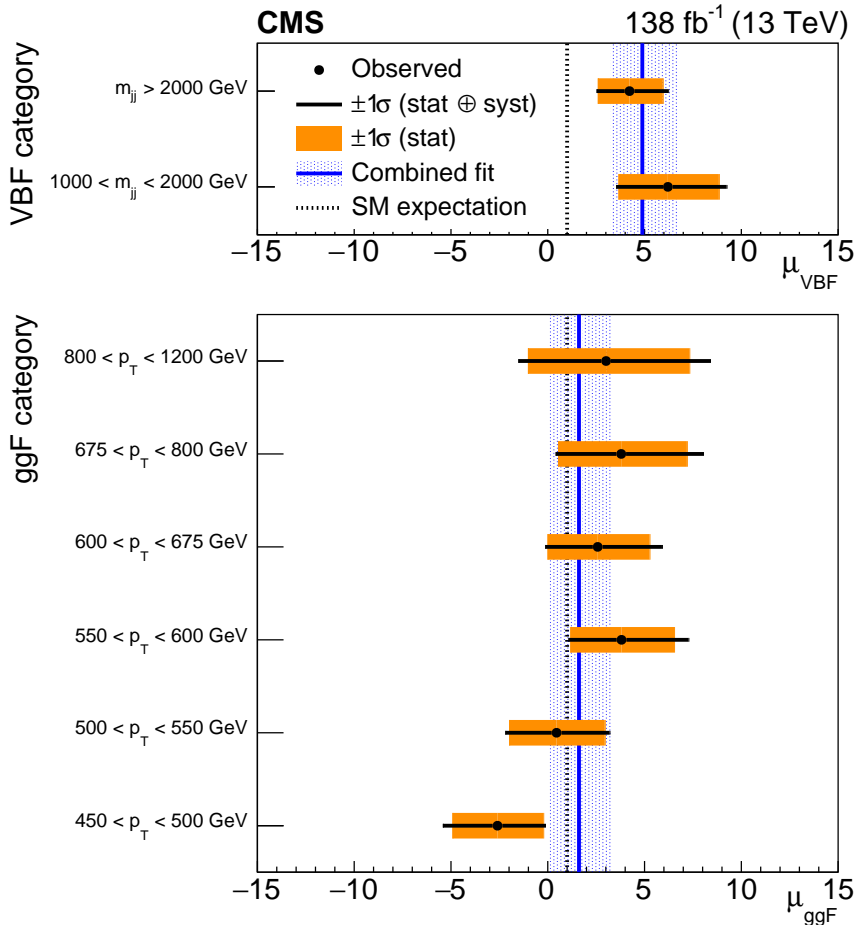


Figure 9: Upper: the VBF signal strength is shown in black, fitted per m_{jj} bin, with the ratio of the ggF and VBF cross sections fixed to the value obtained in the signal strength fit. The horizontal black line represents the total uncertainty, and the orange bar represents the statistical-only component. The combined VBF signal strength and its uncertainty are shown in blue. The SM expectation is shown as a dashed line. Lower: the ggF signal strength is shown in black, fitted per p_{T} bin, with the ratio of the ggF and VBF cross sections fixed to the value obtained in the signal strength fit. The horizontal black line represents the total uncertainty, and the orange bar represents the statistical-only component. The combined ggF signal strength and its uncertainty are shown in blue. The SM expectation is shown as a dashed line.

Table 4. The best fit for the ggF bin with $300 < p_T^{\text{H,gen}} < 450 \text{ GeV}$ lies below zero cross section, as can happen when the signal is estimated with a fit over a large background. However, the uncertainty in this bin is found to be comparatively large due to the limited number of these events passing the analysis selection, and the SM cross section value is well within the uncertainty.

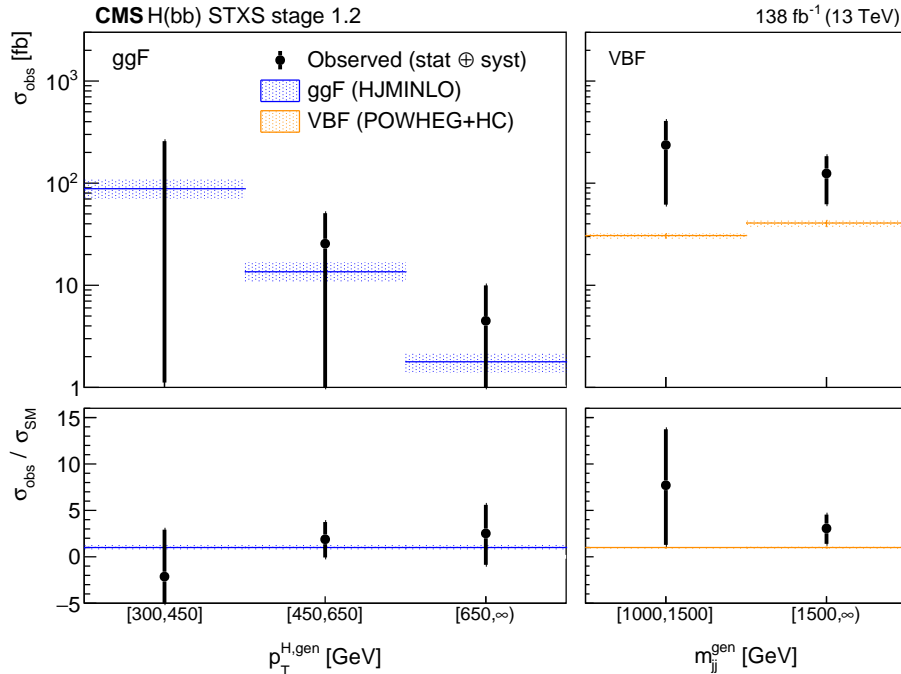


Figure 10: Unfolded cross section in five of the STXS stage 1.2 bins: three bins of Higgs boson p_T in ggF, and two bins of generator-level m_{jj} in VBF. The SM prediction from HJMINLO and POWHEG (plus higher order EW and NNLO QCD corrections) is overlaid for the ggF and VBF production mechanisms, respectively. The lower panel shows the ratio of the measured cross section to the SM prediction.

Table 4: Summary of the best fit estimators for the cross sections. In addition to the listed selection, each fiducial region has a rapidity requirement of $|y^{\text{H,gen}}| < 2.5$. The third column shows the SM predicted cross section and uncertainty. The fourth column shows the fitted cross section, and the final column shows the total uncertainty followed by the statistical component in parentheses.

Process	Fiducial region	σ_{SM} [fb]	σ_{obs} [fb]	Uncertainty [fb]
ggF	$300 < p_T^{\text{H,gen}} < 450 \text{ GeV}$	90 ± 20	-190	$^{+430}_{-450} (\pm 410 \text{ stat})$
ggF	$450 < p_T^{\text{H,gen}} < 650 \text{ GeV}$	14 ± 3	26	$^{+25}_{-27} (\pm 24 \text{ stat})$
ggF	$p_T^{\text{H,gen}} > 650 \text{ GeV}$	2 ± 0.4	4	$^{+6}_{-5} (\pm 5 \text{ stat})$
VBF	$p_T^{\text{H,gen}} > 200 \text{ GeV},$ $1.0 < m_{jj}^{\text{gen}} < 1.5 \text{ TeV}$	31^{+1}_{-2}	240	$^{+200}_{-190} (\pm 170 \text{ stat})$
VBF	$p_T^{\text{H,gen}} > 200 \text{ GeV},$ $m_{jj}^{\text{gen}} > 1.5 \text{ TeV}$	41^{+2}_{-3}	120	$^{+68}_{-61} (\pm 62 \text{ stat})$

8 Summary

A measurement has been performed of boosted Higgs bosons (H) produced via vector boson fusion (VBF) or gluon fusion (ggF) and decaying to bottom quark-antiquark pairs. The analysis goes beyond the inclusive $H \rightarrow b\bar{b}$ measurements performed thus far to provide the first exploration of Higgs bosons produced with high transverse momentum ($p_T > 450$ GeV) in the VBF channel. The signal strengths for both processes are extracted simultaneously by performing a maximum likelihood fit to data in the large-radius jet mass distribution. The observed signal strengths for the VBF and ggF processes are $4.9^{+1.9}_{-1.6}$ and $1.6^{+1.7}_{-1.5}$, corresponding to a 2.7σ difference between data and the standard model expectation. The unfolded simplified template cross sections, which will provide an important input to future combined interpretations of H interactions, are also reported.

Acknowledgments

We congratulate our colleagues in the CERN accelerator departments for the excellent performance of the LHC and thank the technical and administrative staffs at CERN and at other CMS institutes for their contributions to the success of the CMS effort. In addition, we gratefully acknowledge the computing centers and personnel of the Worldwide LHC Computing Grid and other centers for delivering so effectively the computing infrastructure essential to our analyses. Finally, we acknowledge the enduring support for the construction and operation of the LHC, the CMS detector, and the supporting computing infrastructure provided by the following funding agencies: SC (Armenia), BMBWF and FWF (Austria); FNRS and FWO (Belgium); CNPq, CAPES, FAPERJ, FAPERGS, and FAPESP (Brazil); MES and BNSF (Bulgaria); CERN; CAS, MoST, and NSFC (China); MINCIENCIAS (Colombia); MSES and CSF (Croatia); RIF (Cyprus); SENESCYT (Ecuador); ERC PRG, RVT3 and MoER TK202 (Estonia); Academy of Finland, MEC, and HIP (Finland); CEA and CNRS/IN2P3 (France); SRNSF (Georgia); BMBF, DFG, and HGF (Germany); GSRI (Greece); NKFIH (Hungary); DAE and DST (India); IPM (Iran); SFI (Ireland); INFN (Italy); MSIP and NRF (Republic of Korea); MES (Latvia); LMELT (Lithuania); MOE and UM (Malaysia); BUAP, CINVESTAV, CONACYT, LNS, SEP, and UASLP-FAI (Mexico); MOS (Montenegro); MBIE (New Zealand); PAEC (Pakistan); MES and NSC (Poland); FCT (Portugal); MESTD (Serbia); MCIN/AEI and PCTI (Spain); MOSTR (Sri Lanka); Swiss Funding Agencies (Switzerland); MST (Taipei); MHESI and NSTDA (Thailand); TUBITAK and TENMAK (Turkey); NASU (Ukraine); STFC (United Kingdom); DOE and NSF (USA).

Individuals have received support from the Marie-Curie program and the European Research Council and Horizon 2020 Grant, contract Nos. 675440, 724704, 752730, 758316, 765710, 824093, 101115353, 101002207, and COST Action CA16108 (European Union); the Leventis Foundation; the Alfred P. Sloan Foundation; the Alexander von Humboldt Foundation; the Science Committee, project no. 22rl-037 (Armenia); the Belgian Federal Science Policy Office; the Fonds pour la Formation à la Recherche dans l'Industrie et dans l'Agriculture (FRIA-Belgium); the F.R.S.-FNRS and FWO (Belgium) under the “Excellence of Science – EOS” – be.h project n. 30820817; the Beijing Municipal Science & Technology Commission, No. Z191100007219010 and Fundamental Research Funds for the Central Universities (China); the Ministry of Education, Youth and Sports (MEYS) of the Czech Republic; the Shota Rustaveli National Science Foundation, grant FR-22-985 (Georgia); the Deutsche Forschungsgemeinschaft (DFG), among others, under Germany’s Excellence Strategy – EXC 2121 “Quantum Universe” – 390833306, and under project number 400140256 - GRK2497; the Hellenic Foundation for Research and Innovation (HFRI), Project Number 2288 (Greece); the Hungarian Academy of Sciences, the

New National Excellence Program - ÚNKP, the NKFIH research grants K 131991, K 133046, K 138136, K 143460, K 143477, K 146913, K 146914, K 147048, 2020-2.2.1-ED-2021-00181, and TKP2021-NKTA-64 (Hungary); the Council of Science and Industrial Research, India; ICSC – National Research Center for High Performance Computing, Big Data and Quantum Computing and FAIR – Future Artificial Intelligence Research, funded by the NextGenerationEU program (Italy); the Latvian Council of Science; the Ministry of Education and Science, project no. 2022/WK/14, and the National Science Center, contracts Opus 2021/41/B/ST2/01369 and 2021/43/B/ST2/01552 (Poland); the Fundação para a Ciência e a Tecnologia, grant CEECIND/01334/2018 (Portugal); the National Priorities Research Program by Qatar National Research Fund; MCIN/AEI/10.13039/501100011033, ERDF “a way of making Europe”, and the Programa Estatal de Fomento de la Investigación Científica y Técnica de Excelencia María de Maeztu, grant MDM-2017-0765 and Programa Severo Ochoa del Principado de Asturias (Spain); the Chulalongkorn Academic into Its 2nd Century Project Advancement Project, and the National Science, Research and Innovation Fund via the Program Management Unit for Human Resources & Institutional Development, Research and Innovation, grant B39G670016 (Thailand); the Kavli Foundation; the Nvidia Corporation; the SuperMicro Corporation; the Welch Foundation, contract C-1845; and the Weston Havens Foundation (USA).

References

- [1] ATLAS Collaboration, “Observation of a new particle in the search for the standard model Higgs boson with the ATLAS detector at the LHC”, *Phys. Lett. B* **716** (2012) 1, doi:[10.1016/j.physletb.2012.08.020](https://doi.org/10.1016/j.physletb.2012.08.020), arXiv:[1207.7214](https://arxiv.org/abs/1207.7214).
- [2] CMS Collaboration, “Observation of a new boson at a mass of 125 GeV with the CMS experiment at the LHC”, *Phys. Lett. B* **716** (2012) 30, doi:[10.1016/j.physletb.2012.08.021](https://doi.org/10.1016/j.physletb.2012.08.021), arXiv:[1207.7235](https://arxiv.org/abs/1207.7235).
- [3] CMS Collaboration, “Observation of a new boson with mass near 125 GeV in pp collisions at $\sqrt{s} = 7$ and 8 TeV”, *JHEP* **06** (2013) 081, doi:[10.1007/JHEP06\(2013\)081](https://doi.org/10.1007/JHEP06(2013)081), arXiv:[1303.4571](https://arxiv.org/abs/1303.4571).
- [4] CMS Collaboration, “A portrait of the Higgs boson by the CMS experiment ten years after the discovery”, *Nature* **607** (2022) 60, doi:[10.1038/s41586-022-04892-x](https://doi.org/10.1038/s41586-022-04892-x), arXiv:[2207.00043](https://arxiv.org/abs/2207.00043).
- [5] ATLAS Collaboration, “A detailed map of Higgs boson interactions by the ATLAS experiment ten years after the discovery”, *Nature* **607** (2022) 52, doi:[10.1038/s41586-022-04893-w](https://doi.org/10.1038/s41586-022-04893-w), arXiv:[2207.00092](https://arxiv.org/abs/2207.00092).
- [6] ATLAS Collaboration, “Measurements of Higgs boson production and couplings in diboson final states with the ATLAS detector at the LHC”, *Phys. Lett. B* **726** (2013) 88, doi:[10.1016/j.physletb.2013.08.010](https://doi.org/10.1016/j.physletb.2013.08.010), arXiv:[1307.1427](https://arxiv.org/abs/1307.1427).
- [7] A. Salam, “Weak and electromagnetic interactions”, in *Elementary particle physics: relativistic groups and analyticity*, N. Svartholm, ed., p. 367. Almqvist & Wiksell, Stockholm, 1968. Proceedings of the eighth Nobel symposium.
- [8] S. L. Glashow, “Partial-symmetries of weak interactions”, *Nucl. Phys.* **22** (1961) 579, doi:[10.1016/0029-5582\(61\)90469-2](https://doi.org/10.1016/0029-5582(61)90469-2).

- [9] S. Weinberg, “A model of leptons”, *Phys. Rev. Lett.* **19** (1967) 1264, doi:[10.1103/PhysRevLett.19.1264](https://doi.org/10.1103/PhysRevLett.19.1264).
- [10] F. Englert and R. Brout, “Broken symmetry and the mass of gauge vector mesons”, *Phys. Rev. Lett.* **13** (1964) 321, doi:[10.1103/PhysRevLett.13.321](https://doi.org/10.1103/PhysRevLett.13.321).
- [11] P. W. Higgs, “Broken symmetries, massless particles and gauge fields”, *Phys. Rev. Lett.* **12** (1964) 132, doi:[10.1016/0031-9163\(64\)91136-9](https://doi.org/10.1016/0031-9163(64)91136-9).
- [12] P. W. Higgs, “Broken symmetries and the masses of gauge bosons”, *Phys. Rev. Lett.* **13** (1964) 508, doi:[10.1103/PhysRevLett.13.508](https://doi.org/10.1103/PhysRevLett.13.508).
- [13] P. W. Higgs, “Spontaneous symmetry breakdown without massless bosons”, *Phys. Rev. Lett.* **145** (1966) 1156, doi:[10.1103/PhysRev.145.1156](https://doi.org/10.1103/PhysRev.145.1156).
- [14] G. S. Guralnik, C. R. Hagen, and T. W. B. Kibble, “Global conservation laws and massless particles”, *Phys. Rev. Lett.* **13** (1964) 585, doi:[10.1103/PhysRevLett.13.585](https://doi.org/10.1103/PhysRevLett.13.585).
- [15] C. Grojean, E. Salvioni, M. Schlaffer, and A. Weiler, “Very boosted Higgs in gluon fusion”, *JHEP* **05** (2014) 22, doi:[10.1007/jhep05\(2014\)022](https://doi.org/10.1007/jhep05(2014)022), arXiv:[1312.3317](https://arxiv.org/abs/1312.3317).
- [16] M. Schlaffer et al., “Boosted Higgs shapes”, *Eur. Phys. J. C* **74** (2014) 3120, doi:[10.1140/epjc/s10052-014-3120-z](https://doi.org/10.1140/epjc/s10052-014-3120-z), arXiv:[1405.4295](https://arxiv.org/abs/1405.4295).
- [17] S. Dawson, I. M. Lewis, and M. Zeng, “Usefulness of effective field theory for boosted Higgs production”, *Phys. Rev. D* **91** (2015) 074012, doi:[10.1103/physrevd.91.074012](https://doi.org/10.1103/physrevd.91.074012), arXiv:[1501.04103](https://arxiv.org/abs/1501.04103).
- [18] M. Grazzini, A. Ilnicka, M. Spira, and M. Wiesemann, “Modeling BSM effects on the Higgs transverse-momentum spectrum in an EFT approach”, *JHEP* **03** (2017) 115, doi:[10.1007/jhep03\(2017\)115](https://doi.org/10.1007/jhep03(2017)115), arXiv:[1612.00283](https://arxiv.org/abs/1612.00283).
- [19] F. Maltoni, K. Mawatari, and M. Zaro, “Higgs characterisation via vector-boson fusion and associated production: NLO and parton-shower effects”, *Eur. Phys. J. C* **74** (2014) 2710, doi:[10.1140/epjc/s10052-013-2710-5](https://doi.org/10.1140/epjc/s10052-013-2710-5), arXiv:[1311.1829](https://arxiv.org/abs/1311.1829).
- [20] C. Degrande et al., “Electroweak Higgs boson production in the standard model effective field theory beyond leading order in QCD”, *Eur. Phys. J. C* **77** (2017) 262, doi:[10.1140/epjc/s10052-017-4793-x](https://doi.org/10.1140/epjc/s10052-017-4793-x), arXiv:[1609.04833](https://arxiv.org/abs/1609.04833).
- [21] J. R. Andersen et al., “Les Houches 2015: Physics at TeV Colliders Standard Model working group report”, in *Proc. 9th Les Houches Workshop on Physics at TeV Colliders (PhysTeV 2015) Les Houches, France, June 1–19, 2015*. 2016. arXiv:[1605.04692](https://arxiv.org/abs/1605.04692).
- [22] K. Becker et al., “Precise predictions for boosted Higgs production”, *SciPost Phys. Core* **7** (2024) 001, doi:[10.21468/SciPostPhysCore.7.1.001](https://doi.org/10.21468/SciPostPhysCore.7.1.001), arXiv:[2005.07762](https://arxiv.org/abs/2005.07762).
- [23] CMS Collaboration, “Inclusive search for a highly boosted Higgs boson decaying to a bottom quark-antiquark pair”, *Phys. Rev. Lett.* **120** (2018) 071802, doi:[10.1103/physrevlett.120.071802](https://doi.org/10.1103/physrevlett.120.071802), arXiv:[1709.05543](https://arxiv.org/abs/1709.05543).
- [24] ATLAS Collaboration, “Constraints on Higgs boson production with large transverse momentum using $H \rightarrow b\bar{b}$ decays in the ATLAS detector”, *Phys. Rev. D* **105** (2022) 092003, doi:[10.1103/PhysRevD.105.092003](https://doi.org/10.1103/PhysRevD.105.092003), arXiv:[2111.08340](https://arxiv.org/abs/2111.08340).

- [25] CMS Collaboration, “Inclusive search for highly boosted Higgs bosons decaying to bottom quark-antiquark pairs in proton-proton collisions at $\sqrt{s} = 13 \text{ TeV}$ ”, *JHEP* **12** (2020) 085, doi:10.1007/jhep12(2020)085, arXiv:2006.13251.
- [26] ATLAS Collaboration, “Measurement of the associated production of a Higgs boson decaying into b-quarks with a vector boson at high transverse momentum in pp collisions at $\sqrt{s} = 13 \text{ TeV}$ with the ATLAS detector”, *Phys. Lett. B* **816** (2021) 136204, doi:10.1016/j.physletb.2021.136204, arXiv:2008.02508.
- [27] ATLAS Collaboration, “Study of high-momentum Higgs boson production in association with a vector boson in the qqbb final state with the ATLAS detector”, *Phys. Rev. Lett.* **132** (2024) 131802, doi:10.1103/physrevlett.132.131802, arXiv:2312.07605.
- [28] CMS Collaboration, “Measurement of simplified template cross sections of the Higgs boson produced in association with W or Z bosons in the $H \rightarrow b\bar{b}$ decay channel in proton-proton collisions at $\sqrt{s} = 13 \text{ TeV}$ ”, *Phys. Rev. D* **109** (2024) 092011, doi:10.1103/physrevd.109.092011, arXiv:2312.07562.
- [29] CMS Collaboration, “Precision luminosity measurement in proton-proton collisions at $\sqrt{s} = 13 \text{ TeV}$ in 2015 and 2016 at CMS”, *Eur. Phys. J. C* **81** (2021) 800, doi:10.1140/epjc/s10052-021-09538-2, arXiv:2104.01927.
- [30] CMS Collaboration, “CMS luminosity measurement for the 2017 data-taking period at $\sqrt{s} = 13 \text{ TeV}$ ”, CMS Physics Analysis Summary CMS-PAS-LUM-17-004, 2018.
- [31] CMS Collaboration, “CMS luminosity measurement for the 2018 data-taking period at $\sqrt{s} = 13 \text{ TeV}$ ”, CMS Physics Analysis Summary CMS-PAS-LUM-18-002, 2019.
- [32] CMS Collaboration, “Performance of the mass-decorrelated DeepDoubleX classifier for double-b and double-c large-radius jets with the CMS detector”, CMS Detector Performance Note CMS-DP-2022-041, 2022.
- [33] CMS Collaboration, “Performance of deep tagging algorithms for boosted double quark jet topology in proton-proton collisions at 13 TeV with the Phase-0 CMS detector”, CMS Detector Performance Note CMS-DP-2018-046, 2018.
- [34] CMS Collaboration, “Identification of heavy-flavour jets with the CMS detector in pp collisions at 13 TeV”, *JINST* **13** (2018) P05011, doi:10.1088/1748-0221/13/05/P05011, arXiv:1712.07158.
- [35] CMS Collaboration, “The CMS experiment at the CERN LHC”, *JINST* **3** (2008) S08004, doi:10.1088/1748-0221/3/08/S08004.
- [36] CMS Collaboration, “Performance of the CMS level-1 trigger in proton-proton collisions at $\sqrt{s} = 13 \text{ TeV}$ ”, *JINST* **15** (2020) P10017, doi:10.1088/1748-0221/15/10/p10017, arXiv:2006.10165.
- [37] CMS Collaboration, “The CMS trigger system”, *JINST* **12** (2017) P01020, doi:10.1088/1748-0221/12/01/p01020, arXiv:1609.02366.
- [38] CMS Collaboration, “Electron and photon reconstruction and identification with the CMS experiment at the CERN LHC”, *JINST* **16** (2021) P05014, doi:10.1088/1748-0221/16/05/p05014, arXiv:2012.06888.

- [39] CMS Collaboration, “Performance of the CMS muon detector and muon reconstruction with proton-proton collisions at $\sqrt{s} = 13$ TeV”, *JINST* **13** (2018) P06015, doi:10.1088/1748-0221/13/06/p06015, arXiv:1804.04528.
- [40] CMS Collaboration, “Description and performance of track and primary-vertex reconstruction with the CMS tracker”, *JINST* **9** (2014) P10009, doi:10.1088/1748-0221/9/10/p10009, arXiv:1405.6569.
- [41] GEANT4 Collaboration, “GEANT4—a simulation toolkit”, *Nucl. Instrum. Meth. A* **506** (2003) 250, doi:10.1016/S0168-9002(03)01368-8.
- [42] J. Alwall et al., “The automated computation of tree-level and next-to-leading order differential cross sections, and their matching to parton shower simulations”, *JHEP* **07** (2014) 079, doi:10.1007/JHEP07(2014)079, arXiv:1405.0301.
- [43] J. Alwall et al., “Comparative study of various algorithms for the merging of parton showers and matrix elements in hadronic collisions”, *Eur. Phys. J. C* **53** (2007) 473, doi:10.1140/epjc/s10052-007-0490-5, arXiv:0706.2569.
- [44] R. Frederix and S. Frixione, “Merging meets matching in MC@NLO”, *JHEP* **12** (2012) 061, doi:10.1007/JHEP12(2012)061, arXiv:1209.6215.
- [45] S. Kallweit et al., “NLO electroweak automation and precise predictions for W+multijet production at the LHC”, *JHEP* **04** (2015) 012, doi:10.1007/JHEP04(2015)012, arXiv:1412.5157.
- [46] S. Kallweit et al., “NLO QCD+EW predictions for V+jets including off-shell vector-boson decays and multijet merging”, *JHEP* **04** (2016) 021, doi:10.1007/JHEP04(2016)021, arXiv:1511.08692.
- [47] S. Kallweit et al., “NLO QCD+EW automation and precise predictions for V+multijet production”, in *50th Rencontres de Moriond on QCD and High Energy Interactions*, p. 121. 2015. arXiv:1505.05704.
- [48] J. M. Lindert et al., “Precise predictions for V+jets dark matter backgrounds”, *Eur. Phys. J. C* **77** (2017) 829, doi:10.1140/epjc/s10052-017-5389-1, arXiv:1705.04664.
- [49] T. Sjöstrand et al., “An introduction to PYTHIA 8.2”, *Comput. Phys. Commun.* **191** (2015) 159, doi:10.1016/j.cpc.2015.01.024, arXiv:1410.3012.
- [50] J. M. Campbell and R. K. Ellis, “MCFM for the Tevatron and the LHC”, *Nucl. Phys. Proc. Suppl.* **205-206** (2010) 10, doi:10.1016/j.nuclphysbps.2010.08.011, arXiv:1007.3492.
- [51] S. Frixione, P. Nason, and C. Oleari, “Matching NLO QCD computations with parton shower simulations: the POWHEG method”, *JHEP* **11** (2007) 070, doi:10.1088/1126-6708/2007/11/070, arXiv:0709.2092.
- [52] S. Alioli, P. Nason, C. Oleari, and E. Re, “A general framework for implementing NLO calculations in shower Monte Carlo programs: the POWHEG BOX”, *JHEP* **06** (2010) 043, doi:10.1007/JHEP06(2010)043, arXiv:1002.2581.
- [53] S. Frixione, G. Ridolfi, and P. Nason, “A positive-weight next-to-leading-order Monte Carlo for heavy flavour hadroproduction”, *JHEP* **09** (2007) 126, doi:10.1088/1126-6708/2007/09/126, arXiv:0707.3088.

- [54] R. Frederix, E. Re, and P. Torrielli, “Single-top t -channel hadroproduction in the four-flavour scheme with POWHEG and amc@NLO”, *JHEP* **09** (2012) 130, doi:10.1007/JHEP09(2012)130, arXiv:1207.5391.
- [55] E. Re, “Single-top Wt-channel production matched with parton showers using the POWHEG method”, *Eur. Phys. J. C* **71** (2011) 1547, doi:10.1140/epjc/s10052-011-1547-z, arXiv:1009.2450.
- [56] P. F. Monni et al., “MiNNLO_{PS}: a new method to match NNLO QCD to parton showers”, *JHEP* **05** (2020) 143, doi:10.1007/JHEP05(2020)143, arXiv:1908.06987. [Erratum: doi:10.1007/JHEP05(2020)143].
- [57] P. F. Monni, E. Re, and M. Wiesemann, “MiNNLO_{PS}: optimizing $2 \rightarrow 1$ hadronic processes”, *Eur. Phys. J. C* **80** (2020) 1075, doi:10.1140/epjc/s10052-020-08658-5, arXiv:2006.04133.
- [58] T. Neumann, “NLO Higgs+jet production at large transverse momenta including top quark mass effects”, *J. Phys. Commun.* **2** (2018) 095017, doi:10.1088/2399-6528/aadfbf, arXiv:1802.02981.
- [59] P. Nason and C. Oleari, “NLO Higgs boson production via vector-boson fusion matched with shower in POWHEG”, *JHEP* **02** (2010) 037, doi:10.1007/JHEP02(2010)037, arXiv:0911.5299.
- [60] G. Luisoni, P. Nason, C. Oleari, and F. Tramontano, “HW $^\pm$ /HZ+0 and 1 jet at NLO with the POWHEG box interfaced to GoSam and their merging within MiNLO”, *JHEP* **10** (2013) 083, doi:10.1007/JHEP10(2013)083, arXiv:1306.2542.
- [61] H. B. Hartanto, B. Jager, L. Reina, and D. Wackerlo, “Higgs boson production in association with top quarks in the POWHEG BOX”, *Phys. Rev. D* **91** (2015) 094003, doi:10.1103/PhysRevD.91.094003, arXiv:1501.04498.
- [62] M. Cacciari et al., “Fully differential vector-boson-fusion Higgs production at next-to-next-to-leading order”, *Phys. Rev. Lett.* **115** (2015) 082002, doi:10.1103/PhysRevLett.115.082002, arXiv:1506.02660. [Erratum: doi:10.1103/PhysRevLett.120.139901].
- [63] F. A. Dreyer and A. Karlberg, “Vector-boson fusion Higgs production at three loops in QCD”, *Phys. Rev. Lett.* **117** (2016) 072001, doi:10.1103/PhysRevLett.117.072001, arXiv:1606.00840.
- [64] CMS Collaboration, “Extraction and validation of a new set of CMS PYTHIA 8 tunes from underlying-event measurements”, *Eur. Phys. J. C* **80** (2020) 4, doi:10.1140/epjc/s10052-019-7499-4, arXiv:1903.12179.
- [65] NNPDF Collaboration, “Parton distributions from high-precision collider data”, *Eur. Phys. J. C* **77** (2017) 663, doi:10.1140/epjc/s10052-017-5199-5, arXiv:1706.00428.
- [66] CMS Collaboration, “Particle-flow reconstruction and global event description with the CMS detector”, *JINST* **12** (2017) P10003, doi:10.1088/1748-0221/12/10/p10003, arXiv:1706.04965.
- [67] M. Cacciari, G. P. Salam, and G. Soyez, “The anti- k_T jet clustering algorithm”, *JHEP* **04** (2008) 063, doi:10.1088/1126-6708/2008/04/063, arXiv:0802.1189.

- [68] M. Cacciari, G. P. Salam, and G. Soyez, “FastJet User Manual”, *Eur. Phys. J. C* **72** (2012) 1896, doi:[10.1140/epjc/s10052-012-1896-2](https://doi.org/10.1140/epjc/s10052-012-1896-2), arXiv:[1111.6097](https://arxiv.org/abs/1111.6097).
- [69] CMS Collaboration, “Jet algorithms performance in 13 TeV data”, CMS Physics Analysis Summary CMS-PAS-JME-16-003, 2017.
- [70] CMS Collaboration, “Pileup mitigation at CMS in 13 TeV data”, *JINST* **15** (2020) P09018, doi:[10.1088/1748-0221/15/09/P09018](https://doi.org/10.1088/1748-0221/15/09/P09018), arXiv:[2003.00503](https://arxiv.org/abs/2003.00503).
- [71] D. Bertolini, P. Harris, M. Low, and N. Tran, “Pileup Per Particle Identification”, *JHEP* **10** (2014) 059, doi:[10.1007/JHEP10\(2014\)059](https://doi.org/10.1007/JHEP10(2014)059), arXiv:[1407.6013](https://arxiv.org/abs/1407.6013).
- [72] CMS Collaboration, “Jet energy scale and resolution in the CMS experiment in pp collisions at 8 TeV”, *JINST* **12** (2017) P02014, doi:[10.1088/1748-0221/12/02/P02014](https://doi.org/10.1088/1748-0221/12/02/P02014), arXiv:[1607.03663](https://arxiv.org/abs/1607.03663).
- [73] D. Krohn, J. Thaler, and L.-T. Wang, “Jet Trimming”, *JHEP* **02** (2010) 084, doi:[10.1007/JHEP02\(2010\)084](https://doi.org/10.1007/JHEP02(2010)084), arXiv:[0912.1342](https://arxiv.org/abs/0912.1342).
- [74] A. J. Larkoski, S. Marzani, G. Soyez, and J. Thaler, “Soft Drop”, *JHEP* **05** (2014) 146, doi:[10.1007/JHEP05\(2014\)146](https://doi.org/10.1007/JHEP05(2014)146), arXiv:[1402.2657](https://arxiv.org/abs/1402.2657).
- [75] ATLAS Collaboration, “Measurement of soft-drop jet observables in pp collisions with the ATLAS detector at $\sqrt{s} = 13$ TeV”, *Phys. Rev. D* **101** (2020) 052007, doi:[10.1103/physrevd.101.052007](https://doi.org/10.1103/physrevd.101.052007), arXiv:[1912.09837](https://arxiv.org/abs/1912.09837).
- [76] I. Moult, L. Necib, and J. Thaler, “New Angles on Energy Correlation Functions”, *JHEP* **12** (2016) 153, doi:[10.1007/JHEP12\(2016\)153](https://doi.org/10.1007/JHEP12(2016)153), arXiv:[1609.07483](https://arxiv.org/abs/1609.07483).
- [77] J. Dolen et al., “Thinking outside the ROCs: Designing Decorrelated Taggers (DDT) for jet substructure”, *JHEP* **05** (2016) 156, doi:[10.1007/JHEP05\(2016\)156](https://doi.org/10.1007/JHEP05(2016)156), arXiv:[1603.00027](https://arxiv.org/abs/1603.00027).
- [78] E. Bols et al., “Jet flavour classification using DeepJet”, *JINST* **15** (2020) P12012, doi:[10.1088/1748-0221/15/12/P12012](https://doi.org/10.1088/1748-0221/15/12/P12012), arXiv:[2008.10519](https://arxiv.org/abs/2008.10519).
- [79] CMS Collaboration, “Performance of the DeepJet b tagging algorithm using 41.9/fb of data from proton-proton collisions at 13 TeV with Phase 1 CMS detector”, CMS Detector Performance Note CMS-DP-2018-058, 2018.
- [80] CMS Collaboration, “Performance of missing transverse momentum reconstruction in proton-proton collisions at $\sqrt{s} = 13$ TeV using the CMS detector”, *JINST* **14** (2019) P07004, doi:[10.1088/1748-0221/14/07/P07004](https://doi.org/10.1088/1748-0221/14/07/P07004), arXiv:[1903.06078](https://arxiv.org/abs/1903.06078).
- [81] CMS Collaboration, “Performance of reconstruction and identification of τ leptons decaying to hadrons and ν_τ in pp collisions at $\sqrt{s} = 13$ TeV”, *JINST* **13** (2018) P10005, doi:[10.1088/1748-0221/13/10/p10005](https://doi.org/10.1088/1748-0221/13/10/p10005), arXiv:[1809.02816](https://arxiv.org/abs/1809.02816).
- [82] CMS Collaboration, “Identification of hadronic tau lepton decays using a deep neural network”, *JINST* **17** (2022) P07023, doi:[10.1088/1748-0221/17/07/p07023](https://doi.org/10.1088/1748-0221/17/07/p07023), arXiv:[2201.08458](https://arxiv.org/abs/2201.08458).
- [83] R. A. Fisher, “On the interpretation of χ^2 from contingency tables, and the calculation of P”, *J. R. Stat. Soc.* **85** (1922) 87, doi:[10.2307/2340521](https://doi.org/10.2307/2340521).

- [84] E. Gross and O. Vitells, “Trial factors for the look elsewhere effect in high energy physics”, *Eur. Phys. J. C* **70** (2010) 525, doi:10.1140/epjc/s10052-010-1470-8, arXiv:1005.1891.
- [85] J. S. Conway, “Incorporating Nuisance Parameters in Likelihoods for Multisource Spectra”, in *Proceedings of the PHYSTAT 2011 Workshop on Statistical Issues Related to Discovery Claims in Search Experiments and Unfolding*, p. 115. 2011. arXiv:1103.0354. doi:10.5170/CERN-2011-006.115.
- [86] CMS Collaboration, “Performance of heavy-flavour jet identification in boosted topologies in proton-proton collisions at $\sqrt{s} = 13$ TeV”, Technical Report CMS-PAS-BTV-22-001, 2023.
- [87] CMS Collaboration, “Determination of jet energy calibration and transverse momentum resolution in CMS”, *JINST* **6** (2011) P11002, doi:10.1088/1748-0221/6/11/p11002, arXiv:1107.4277.
- [88] S. Mrenna and P. Skands, “Automated Parton-Shower Variations in PYTHIA 8”, *Phys. Rev. D* **94** (2016) 074005, doi:10.1103/PhysRevD.94.074005, arXiv:1605.08352.
- [89] J. Butterworth et al., “PDF4LHC recommendations for LHC Run II”, *J. Phys. G* **43** (2016) 023001, doi:10.1088/0954-3899/43/2/023001, arXiv:1510.03865.
- [90] ATLAS and CMS Collaborations, and LHC Higgs Combination Group, “Procedure for the LHC Higgs boson search combination in Summer 2011”, Technical Report CMS-NOTE-2011-005, ATL-PHYS-PUB-2011-11, 2011.
- [91] CMS Collaboration, “Precise determination of the mass of the Higgs boson and tests of compatibility of its couplings with the standard model predictions using proton collisions at 7 and 8 TeV”, *Eur. Phys. J. C* **75** (2015) 212, doi:10.1140/epjc/s10052-015-3351-7, arXiv:1412.8662.
- [92] “HEPData record for this analysis”, 2024. doi:10.17182/hepdata.150995.
- [93] CMS Collaboration, “Measurement and interpretation of differential cross sections for Higgs boson production at $\sqrt{s} = 13$ TeV”, *Phys. Lett. B* **792** (2019) 369, doi:10.1016/j.physletb.2019.03.059, arXiv:1812.06504.
- [94] LHC Higgs Cross Section Working Group, “Handbook of LHC Higgs Cross Sections: 4. Deciphering the Nature of the Higgs sector”, 2016. arXiv:1610.07922.

A The CMS Collaboration

Yerevan Physics Institute, Yerevan, Armenia

A. Hayrapetyan, A. Tumasyan¹ 

Institut für Hochenergiephysik, Vienna, Austria

W. Adam , J.W. Andrejkovic, T. Bergauer , S. Chatterjee , K. Damanakis , M. Dragicevic , P.S. Hussain , M. Jeitler² , N. Krammer , A. Li , D. Liko , I. Mikulec , J. Schieck² , R. Schöfbeck , D. Schwarz , M. Sonawane , S. Templ , W. Waltenberger , C.-E. Wulz² 

Universiteit Antwerpen, Antwerpen, Belgium

M.R. Darwish³ , T. Janssen , P. Van Mechelen 

Vrije Universiteit Brussel, Brussel, Belgium

E.S. Bols , J. D'Hondt , S. Dansana , A. De Moor , M. Delcourt , H. El Faham , S. Lowette , I. Makarenko , D. Müller , S. Tavernier , M. Tytgat⁴ , G.P. Van Onsem , S. Van Putte , D. Vannerom 

Université Libre de Bruxelles, Bruxelles, Belgium

B. Clerbaux , A.K. Das, G. De Lentdecker , H. Evard , L. Favart , P. Gianneios , D. Hohov , J. Jaramillo , A. Khalilzadeh, F.A. Khan , K. Lee , M. Mahdavikhorrami , A. Malara , S. Paredes , L. Thomas , M. Vanden Bemden , C. Vander Velde , P. Vanlaer 

Ghent University, Ghent, Belgium

M. De Coen , D. Dobur , Y. Hong , J. Knolle , L. Lambrecht , G. Mestdach, K. Mota Amarilo , C. Rendón, A. Samalan, K. Skovpen , N. Van Den Bossche , J. van der Linden , L. Wezenbeek 

Université Catholique de Louvain, Louvain-la-Neuve, Belgium

A. Benecke , A. Bethani , G. Bruno , C. Caputo , C. Delaere , I.S. Donertas , A. Giammanco , Sa. Jain , V. Lemaitre, J. Lidrych , P. Mastrapasqua , K. Mondal , T.T. Tran , S. Wertz 

Centro Brasileiro de Pesquisas Fisicas, Rio de Janeiro, Brazil

G.A. Alves , E. Coelho , C. Hensel , T. Menezes De Oliveira , A. Moraes , P. Rebello Teles , M. Soeiro

Universidade do Estado do Rio de Janeiro, Rio de Janeiro, Brazil

W.L. Aldá Júnior , M. Alves Gallo Pereira , M. Barroso Ferreira Filho , H. Brandao Malbouisson , W. Carvalho , J. Chinellato⁵, E.M. Da Costa , G.G. Da Silveira⁶ , D. De Jesus Damiao , S. Fonseca De Souza , R. Gomes De Souza, J. Martins⁷ , C. Mora Herrera , L. Mundim , H. Nogima , J.P. Pinheiro , A. Santoro , A. Sznajder , M. Thiel , A. Vilela Pereira 

Universidade Estadual Paulista, Universidade Federal do ABC, São Paulo, Brazil

C.A. Bernardes⁶ , L. Calligaris , T.R. Fernandez Perez Tomei , E.M. Gregores , P.G. Mercadante , S.F. Novaes , B. Orzari , Sandra S. Padula 

Institute for Nuclear Research and Nuclear Energy, Bulgarian Academy of Sciences, Sofia, Bulgaria

A. Aleksandrov , G. Antchev , R. Hadjiiska , P. Iaydjiev , M. Misheva , M. Shopova , G. Sultanov 

University of Sofia, Sofia, Bulgaria

A. Dimitrov , L. Litov , B. Pavlov , P. Petkov , A. Petrov , E. Shumka 

Instituto De Alta Investigación, Universidad de Tarapacá, Casilla 7 D, Arica, Chile

S. Keshri , S. Thakur 

Beihang University, Beijing, China

T. Cheng , T. Javaid , L. Yuan 

Department of Physics, Tsinghua University, Beijing, China

Z. Hu , J. Liu, K. Yi^{8,9} 

Institute of High Energy Physics, Beijing, China

G.M. Chen¹⁰ , H.S. Chen¹⁰ , M. Chen¹⁰ , F. Iemmi , C.H. Jiang, A. Kapoor¹¹ , H. Liao , Z.-A. Liu¹² , R. Sharma¹³ , J.N. Song¹², J. Tao , C. Wang¹⁰, J. Wang , Z. Wang¹⁰, H. Zhang 

State Key Laboratory of Nuclear Physics and Technology, Peking University, Beijing, China

A. Agapitos , Y. Ban , A. Levin , C. Li , Q. Li , Y. Mao, S.J. Qian , X. Sun , D. Wang , H. Yang, L. Zhang , C. Zhou 

Sun Yat-Sen University, Guangzhou, China

Z. You 

University of Science and Technology of China, Hefei, China

K. Jaffel , N. Lu 

Nanjing Normal University, Nanjing, China

G. Bauer¹⁴

Institute of Modern Physics and Key Laboratory of Nuclear Physics and Ion-beam Application (MOE) - Fudan University, Shanghai, China

X. Gao¹⁵ , D. Leggat, H. Okawa 

Zhejiang University, Hangzhou, Zhejiang, China

Z. Lin , C. Lu , M. Xiao 

Universidad de Los Andes, Bogota, Colombia

C. Avila , D.A. Barbosa Trujillo, A. Cabrera , C. Florez , J. Fraga , J.A. Reyes Vega

Universidad de Antioquia, Medellin, Colombia

J. Mejia Guisao , F. Ramirez , M. Rodriguez , J.D. Ruiz Alvarez 

University of Split, Faculty of Electrical Engineering, Mechanical Engineering and Naval Architecture, Split, Croatia

D. Giljanovic , N. Godinovic , D. Lelas , A. Sculac 

University of Split, Faculty of Science, Split, Croatia

M. Kovac , T. Sculac 

Institute Rudjer Boskovic, Zagreb, Croatia

P. Bargassa , V. Brigljevic , B.K. Chitroda , D. Ferencek , K. Jakovcic, S. Mishra , A. Starodumov¹⁶ , T. Susa 

University of Cyprus, Nicosia, Cyprus

A. Attikis , K. Christoforou , S. Konstantinou , J. Mousa , C. Nicolaou, F. Ptochos , P.A. Razis , H. Rykaczewski, H. Saka , A. Stepennov 

Charles University, Prague, Czech RepublicM. Finger , M. Finger Jr. , A. Kveton **Escuela Politecnica Nacional, Quito, Ecuador**E. Ayala **Universidad San Francisco de Quito, Quito, Ecuador**E. Carrera Jarrin **Academy of Scientific Research and Technology of the Arab Republic of Egypt, Egyptian Network of High Energy Physics, Cairo, Egypt**A.A. Abdelalim^{17,18} , E. Salama^{19,20} **Center for High Energy Physics (CHEP-FU), Fayoum University, El-Fayoum, Egypt**M. Abdullah Al-Mashad , M.A. Mahmoud **National Institute of Chemical Physics and Biophysics, Tallinn, Estonia**K. Ehataht , M. Kadastik, T. Lange , S. Nandan , C. Nielsen , J. Pata , M. Raidal , L. Tani , C. Veelken **Department of Physics, University of Helsinki, Helsinki, Finland**H. Kirschenmann , K. Osterberg , M. Voutilainen **Helsinki Institute of Physics, Helsinki, Finland**S. Bharthuar , E. Brücke , F. Garcia , K.T.S. Kallonen , R. Kinnunen, T. Lampén , K. Lassila-Perini , S. Lehti , T. Lindén , L. Martikainen , M. Myllymäki , M.m. Rantanen , H. Siikonen , E. Tuominen , J. Tuominiemi **Lappeenranta-Lahti University of Technology, Lappeenranta, Finland**P. Luukka , H. Petrow **IRFU, CEA, Université Paris-Saclay, Gif-sur-Yvette, France**M. Besancon , F. Couderc , M. Dejardin , D. Denegri, J.L. Faure, F. Ferri , S. Ganjour , P. Gras , G. Hamel de Monchenault , V. Lohezic , J. Malcles , J. Rander, A. Rosowsky , M.Ö. Sahin , A. Savoy-Navarro²¹ , P. Simkina , M. Titov , M. Tornago **Laboratoire Leprince-Ringuet, CNRS/IN2P3, Ecole Polytechnique, Institut Polytechnique de Paris, Palaiseau, France**C. Baldenegro Barrera , F. Beaudette , A. Buchot Perraguin , P. Busson , A. Cappati , C. Charlot , M. Chiusi , F. Damas , O. Davignon , A. De Wit , B.A. Fontana Santos Alves , S. Ghosh , A. Gilbert , R. Granier de Cassagnac , A. Hakimi , B. Harikrishnan , L. Kalipoliti , G. Liu , J. Motta , M. Nguyen , C. Ochando , L. Portales , R. Salerno , J.B. Sauvan , Y. Sirois , A. Tarabini , E. Vernazza , A. Zabi , A. Zghiche **Université de Strasbourg, CNRS, IPHC UMR 7178, Strasbourg, France**J.-L. Agram²² , J. Andrea , D. Apparu , D. Bloch , J.-M. Brom , E.C. Chabert , C. Collard , S. Falke , U. Goerlach , C. Grimaud, R. Haeberle , A.-C. Le Bihan , M. Meena , G. Saha , M.A. Sessini , P. Van Hove **Institut de Physique des 2 Infinis de Lyon (IP2I), Villeurbanne, France**S. Beauceron , B. Blancon , G. Boudoul , N. Chanon , J. Choi , D. Contardo , P. Depasse , C. Dozen²³ , H. El Mamouni, J. Fay , S. Gascon , M. Gouzevitch , C. Greenberg, G. Grenier , B. Ille , I.B. Laktineh, M. Lethuillier , L. Mirabito, S. Perries, A. Purohit , M. Vander Donckt , P. Verdier , J. Xiao 

Georgian Technical University, Tbilisi, GeorgiaG. Adamov, I. Lomidze , Z. Tsamalaidze¹⁶ **RWTH Aachen University, I. Physikalisches Institut, Aachen, Germany**V. Botta , L. Feld , K. Klein , M. Lipinski , D. Meuser , A. Pauls , N. Röwert , M. Teroerde **RWTH Aachen University, III. Physikalisches Institut A, Aachen, Germany**S. Diekmann , A. Dodonova , N. Eich , D. Eliseev , F. Engelke , J. Erdmann , M. Erdmann , P. Fackeldey , B. Fischer , T. Hebbeker , K. Hoepfner , F. Ivone , A. Jung , M.y. Lee , F. Mausolf , M. Merschmeyer , A. Meyer , S. Mukherjee , D. Noll , F. Nowotny, A. Pozdnyakov , Y. Rath, W. Redjeb , F. Rehm, H. Reithler , U. Sarkar , V. Sarkisovi , A. Schmidt , A. Sharma , J.L. Spah , A. Stein , F. Torres Da Silva De Araujo²⁴ , L. Vigilante, S. Wiedenbeck , S. Zaleski**RWTH Aachen University, III. Physikalisches Institut B, Aachen, Germany**C. Dziwok , G. Flügge , W. Haj Ahmad²⁵ , T. Kress , A. Nowack , O. Pooth , A. Stahl , T. Ziemons , A. Zottz **Deutsches Elektronen-Synchrotron, Hamburg, Germany**H. Aarup Petersen , M. Aldaya Martin , J. Alimena , S. Amoroso, Y. An , S. Baxter , M. Bayatmakou , H. Becerril Gonzalez , O. Behnke , A. Belvedere , S. Bhattacharya , F. Blekman²⁶ , K. Borras²⁷ , A. Campbell , A. Cardini , C. Cheng, F. Colombina , S. Consuegra Rodríguez , G. Correia Silva , M. De Silva , G. Eckerlin, D. Eckstein , L.I. Estevez Banos , O. Filatov , E. Gallo²⁶ , A. Geiser , A. Giraldi , V. Guglielmi , M. Guthoff , A. Hinzmann , A. Jafari²⁸ , L. Jeppe , N.Z. Jomhari , B. Kaech , M. Kasemann , C. Kleinwort , R. Kogler , M. Komm , D. Krücker , W. Lange, D. Leyva Pernia , K. Lipka²⁹ , W. Lohmann³⁰ , R. Mankel , I.-A. Melzer-Pellmann , M. Mendizabal Morentin , A.B. Meyer , G. Milella , A. Mussgiller , L.P. Nair , A. Nürnberg , Y. Otarid , J. Park , D. Pérez Adán , E. Ranken , A. Raspereza , B. Ribeiro Lopes , J. Rübenach, A. Saggio , M. Scham^{31,27} , S. Schnake²⁷ , P. Schütze , C. Schwanenberger²⁶ , D. Selivanova , K. Sharko , M. Shchedrolosiev , R.E. Sosa Riccardo , D. Stafford, F. Vazzoler , A. Ventura Barroso , R. Walsh , Q. Wang , Y. Wen , K. Wichmann, L. Wiens²⁷ , C. Wissing , Y. Yang , A. Zimermann Castro Santos **University of Hamburg, Hamburg, Germany**A. Albrecht , S. Albrecht , M. Antonello , S. Bein , L. Benato , S. Bollweg, M. Bonanomi , P. Connor , M. Eich, K. El Morabit , Y. Fischer , C. Garbers , E. Garutti , A. Grohsjean , J. Haller , H.R. Jabusch , G. Kasieczka , P. Keicher, R. Klanner , W. Korcari , T. Kramer , V. Kutzner , F. Labe , J. Lange , A. Lobanov , C. Matthies , A. Mehta , L. Moureaux , M. Mrowietz, A. Nigamova , Y. Nissan, A. Paasch , K.J. Pena Rodriguez , T. Quadfasel , B. Raciti , M. Rieger , D. Savoiu , J. Schindler , P. Schleper , M. Schröder , J. Schwandt , M. Sommerhalder , H. Stadie , G. Steinbrück , A. Tews, M. Wolf **Karlsruher Institut fuer Technologie, Karlsruhe, Germany**S. Brommer , M. Burkart, E. Butz , T. Chwalek , A. Dierlamm , A. Droll, N. Faltermann , M. Giffels , A. Gottmann , F. Hartmann³² , R. Hofsaess , M. Horzela , U. Husemann , J. Kieseler , M. Klute , R. Koppenhöfer , J.M. Lawhorn , M. Link, A. Lintuluoto , S. Maier , S. Mitra , M. Mormile , Th. Müller , M. Neukum, M. Oh , E. Pfeffer , M. Presilla , G. Quast , K. Rabbertz , B. Regnery , N. Shadskiy , I. Shvetsov , H.J. Simonis , M. Toms , N. Trevisani , R.F. Von Cube , M. Wassmer 

S. Wieland [id](#), F. Wittig, R. Wolf [id](#), X. Zuo [id](#)

Institute of Nuclear and Particle Physics (INPP), NCSR Demokritos, Aghia Paraskevi, Greece

G. Anagnostou, G. Daskalakis [id](#), A. Kyriakis, A. Papadopoulos³², A. Stakia [id](#)

National and Kapodistrian University of Athens, Athens, Greece

P. Kontaxakis [id](#), G. Melachroinos, A. Panagiotou, I. Papavergou [id](#), I. Paraskevas [id](#), N. Saoulidou [id](#), K. Theofilatos [id](#), E. Tziaferi [id](#), K. Vellidis [id](#), I. Zisopoulos [id](#)

National Technical University of Athens, Athens, Greece

G. Bakas [id](#), T. Chatzistavrou, G. Karapostoli [id](#), K. Kousouris [id](#), I. Papakrivopoulos [id](#), E. Siamarkou, G. Tsipolitis [id](#), A. Zacharopoulou

University of Ioánnina, Ioánnina, Greece

K. Adamidis, I. Bestintzanos, I. Evangelou [id](#), C. Foudas, C. Kamtsikis, P. Katsoulis, P. Kokkas [id](#), P.G. Kosmoglou Kioseoglou [id](#), N. Manthos [id](#), I. Papadopoulos [id](#), J. Strologas [id](#)

HUN-REN Wigner Research Centre for Physics, Budapest, Hungary

M. Bartók³³ [id](#), C. Hajdu [id](#), D. Horvath^{34,35} [id](#), K. Márton, F. Sikler [id](#), V. Veszpremi [id](#)

MTA-ELTE Lendület CMS Particle and Nuclear Physics Group, Eötvös Loránd University, Budapest, Hungary

M. Csand [id](#), K. Farkas [id](#), M.M.A. Gadallah³⁶ [id](#), . Kadlecik [id](#), P. Major [id](#), K. Mandal [id](#), G. Pasztor [id](#), A.J. Rdl³⁷ [id](#), G.I. Veres [id](#)

Faculty of Informatics, University of Debrecen, Debrecen, Hungary

P. Raics, B. Ujvari [id](#), G. Zilizi [id](#)

Institute of Nuclear Research ATOMKI, Debrecen, Hungary

G. Bencze, S. Czellar, J. Molnar, Z. Szillasi

Karoly Robert Campus, MATE Institute of Technology, Gyongyos, Hungary

T. Csorgo³⁷ [id](#), F. Nemes³⁷ [id](#), T. Novak [id](#)

Panjab University, Chandigarh, India

J. Babbar [id](#), S. Bansal [id](#), S.B. Beri, V. Bhatnagar [id](#), G. Chaudhary [id](#), S. Chauhan [id](#), N. Dhingra³⁸ [id](#), A. Kaur [id](#), A. Kaur [id](#), H. Kaur [id](#), M. Kaur [id](#), S. Kumar [id](#), K. Sandeep [id](#), T. Sheokand, J.B. Singh [id](#), A. Singla [id](#)

University of Delhi, Delhi, India

A. Ahmed [id](#), A. Bhardwaj [id](#), A. Chhetri [id](#), B.C. Choudhary [id](#), A. Kumar [id](#), A. Kumar [id](#), M. Naimuddin [id](#), K. Ranjan [id](#), S. Saumya [id](#)

Saha Institute of Nuclear Physics, HBNI, Kolkata, India

S. Baradia [id](#), S. Barman³⁹ [id](#), S. Bhattacharya [id](#), S. Dutta [id](#), S. Dutta, S. Sarkar

Indian Institute of Technology Madras, Madras, India

M.M. Ameen [id](#), P.K. Behera [id](#), S.C. Behera [id](#), S. Chatterjee [id](#), P. Jana [id](#), P. Kalbhor [id](#), J.R. Komaragiri⁴⁰ [id](#), D. Kumar⁴⁰ [id](#), P.R. Pujahari [id](#), N.R. Saha [id](#), A. Sharma [id](#), A.K. Sikdar [id](#), S. Verma [id](#)

Tata Institute of Fundamental Research-A, Mumbai, India

S. Dugad, M. Kumar [id](#), G.B. Mohanty [id](#), P. Suryadevara

Tata Institute of Fundamental Research-B, Mumbai, India

A. Bala [id](#), S. Banerjee [id](#), R.M. Chatterjee, R.K. Dewanjee⁴¹ [id](#), M. Guchait [id](#), Sh. Jain [id](#),

A. Jaiswal, S. Karmakar , S. Kumar , G. Majumder , K. Mazumdar , S. Parolia , A. Thachayath 

National Institute of Science Education and Research, An OCC of Homi Bhabha National Institute, Bhubaneswar, Odisha, India

S. Bahinipati⁴² , C. Kar , D. Maity⁴³ , P. Mal , T. Mishra , V.K. Muraleedharan Nair Bindhu⁴³ , K. Naskar⁴³ , A. Nayak⁴³ , P. Sadangi, P. Saha , S.K. Swain , S. Varghese⁴³ , D. Vats⁴³ 

Indian Institute of Science Education and Research (IISER), Pune, India

S. Acharya⁴⁴ , A. Alpana , S. Dube , B. Gomber⁴⁴ , B. Kansal , A. Laha , B. Sahu⁴⁴ , S. Sharma , K.Y. Vaish 

Isfahan University of Technology, Isfahan, Iran

H. Bakhshiansohi⁴⁵ , E. Khazaie⁴⁶ , M. Zeinali⁴⁷ 

Institute for Research in Fundamental Sciences (IPM), Tehran, Iran

S. Chenarani⁴⁸ , S.M. Etesami , M. Khakzad , M. Mohammadi Najafabadi 

University College Dublin, Dublin, Ireland

M. Grunewald 

INFN Sezione di Bari^a, Università di Bari^b, Politecnico di Bari^c, Bari, Italy

M. Abbrescia^{a,b} , R. Aly^{a,c,17} , A. Colaleo^{a,b} , D. Creanza^{a,c} , B. D'Anzi^{a,b} , N. De Filippis^{a,c} , M. De Palma^{a,b} , A. Di Florio^{a,c} , W. Elmetenawee^{a,b,17} , L. Fiore^a , G. Iaselli^{a,c} , M. Louka^{a,b} , G. Maggi^{a,c} , M. Maggi^a , I. Margjeka^{a,b} , V. Mastrapasqua^{a,b} , S. My^{a,b} , S. Nuzzo^{a,b} , A. Pellecchia^{a,b} , A. Pompili^{a,b} , G. Pugliese^{a,c} , R. Radogna^a , G. Ramirez-Sanchez^{a,c} , D. Ramos^a , A. Ranieri^a , L. Silvestris^a , F.M. Simone^{a,b} , Ü. Sözbilir^a , A. Stamerra^a , R. Venditti^a , P. Verwilligen^a , A. Zaza^{a,b}

INFN Sezione di Bologna^a, Università di Bologna^b, Bologna, Italy

G. Abbiendi^a , C. Battilana^{a,b} , D. Bonacorsi^{a,b} , L. Borgonovi^a , R. Campanini^{a,b} , P. Capiluppi^{a,b} , A. Castro^{a,b} , F.R. Cavallo^a , G.M. Dallavalle^a , T. Diotalevi^{a,b} , F. Fabbri^a , A. Fanfani^{a,b} , D. Fasanella^{a,b} , P. Giacomelli^a , L. Giommi^{a,b} , C. Grandi^a , L. Guiducci^{a,b} , S. Lo Meo^{a,49} , L. Lunerti^{a,b} , S. Marcellini^a , G. Masetti^a , F.L. Navarra^{a,b} , A. Perrotta^a , F. Primavera^{a,b} , A.M. Rossi^{a,b} , T. Rovelli^{a,b} , G.P. Siroli^{a,b}

INFN Sezione di Catania^a, Università di Catania^b, Catania, Italy

S. Costa^{a,b,50} , A. Di Mattia^a , R. Potenza^{a,b} , A. Tricomi^{a,b,50} , C. Tuve^{a,b} 

INFN Sezione di Firenze^a, Università di Firenze^b, Firenze, Italy

P. Assiouras^a , G. Barbagli^a , G. Bardelli^{a,b} , B. Camaiani^{a,b} , A. Cassesese^a , R. Ceccarelli^a , V. Ciulli^{a,b} , C. Civinini^a , R. D'Alessandro^{a,b} , E. Focardi^{a,b} , T. Kello^a, G. Latino^{a,b} , P. Lenzi^{a,b} , M. Lizzo^a , M. Meschini^a , S. Paoletti^a , A. Papanastassiou^{a,b} , G. Sguazzoni^a , L. Viliani^a 

INFN Laboratori Nazionali di Frascati, Frascati, Italy

L. Benussi , S. Bianco , S. Meola⁵¹ , D. Piccolo 

INFN Sezione di Genova^a, Università di Genova^b, Genova, Italy

P. Chatagnon^a , F. Ferro^a , E. Robutti^a , S. Tosi^{a,b} 

INFN Sezione di Milano-Bicocca^a, Università di Milano-Bicocca^b, Milano, Italy

A. Benaglia^a , G. Boldrini^{a,b} , F. Brivio^a , F. Cetorelli^a , F. De Guio^{a,b} , M.E. Dinardo^{a,b} , P. Dini^a , S. Gennai^a , R. Gerosa^{a,b} , A. Ghezzi^{a,b} , P. Govoni^{a,b} , L. Guzzi^a , M.T. Lucchini^{a,b} , M. Malberti^a , S. Malvezzi^a , A. Massironi^a , D. Menasce^a , L. Moroni^a , M. Paganoni^{a,b} , D. Pedrini^a , B.S. Pinolini^a, S. Ragazzi^{a,b} , T. Tabarelli de Fatis^{a,b} , D. Zuolo^a

INFN Sezione di Napoli^a, Università di Napoli 'Federico II'^b, Napoli, Italy; Università della Basilicata^c, Potenza, Italy; Scuola Superiore Meridionale (SSM)^d, Napoli, Italy

S. Buontempo^a , A. Cagnotta^{a,b} , F. Carnevali^{a,b} , N. Cavallo^{a,c} , F. Fabozzi^{a,c} , A.O.M. Iorio^{a,b} , L. Lista^{a,b,⁵²} , P. Paolucci^{a,³²} , B. Rossi^a , C. Sciacca^{a,b} 

INFN Sezione di Padova^a, Università di Padova^b, Padova, Italy; Università di Trento^c, Trento, Italy

R. Ardino^a , P. Azzi^a , N. Bacchetta^{a,⁵³} , D. Bisello^{a,b} , P. Bortignon^a , G. Bortolato^{a,b} , A. Bragagnolo^{a,b} , R. Carlin^{a,b} , T. Dorigo^a , S. Fantinel^a , F. Fanzago^a , F. Gasparini^{a,b} , U. Gasparini^{a,b} , E. Lusiani^a , M. Margoni^{a,b} , F. Marini^a , A.T. Meneguzzo^{a,b} , M. Migliorini^{a,b} , J. Pazzini^{a,b} , P. Ronchese^{a,b} , R. Rossin^{a,b} , F. Simonetto^{a,b} , G. Strong^a , M. Tosi^{a,b} , A. Triossi^{a,b} , H. Yarar^{a,b} , M. Zanetti^{a,b} , P. Zotto^{a,b} , A. Zucchetta^{a,b} , G. Zumerle^{a,b}

INFN Sezione di Pavia^a, Università di Pavia^b, Pavia, Italy

S. Abu Zeid^{a,²⁰} , C. Aimè^{a,b} , A. Braghieri^a , S. Calzaferri^a , D. Fiorina^a , P. Montagna^{a,b} , V. Re^a , C. Riccardi^{a,b} , P. Salvini^a , I. Vai^{a,b} , P. Vitulo^{a,b} 

INFN Sezione di Perugia^a, Università di Perugia^b, Perugia, Italy

S. Ajmal^{a,b} , G.M. Bilei^a , D. Ciangottini^{a,b} , L. Fanò^{a,b} , M. Magherini^{a,b} , G. Mantovani^{a,b} , V. Mariani^{a,b} , M. Menichelli^a , F. Moscatelli^{a,⁵⁴} , A. Rossi^{a,b} , A. Santocchia^{a,b} , D. Spiga^a , T. Tedeschi^{a,b} 

INFN Sezione di Pisa^a, Università di Pisa^b, Scuola Normale Superiore di Pisa^c, Pisa, Italy; Università di Siena^d, Siena, Italy

P. Asenov^{a,b} , P. Azzurri^a , G. Bagliesi^a , R. Bhattacharya^a , L. Bianchini^{a,b} , T. Boccali^a , E. Bossini^a , D. Bruschini^{a,c} , R. Castaldi^a , M.A. Ciocci^{a,b} , M. Cipriani^{a,b} , V. D'Amante^{a,d} , R. Dell'Orso^a , S. Donato^a , A. Giassi^a , F. Ligabue^{a,c} , D. Matos Figueiredo^a , A. Messineo^{a,b} , M. Musich^{a,b} , F. Palla^a , A. Rizzi^{a,b} , G. Rolandi^{a,c} , S. Roy Chowdhury^a , T. Sarkar^a , A. Scribano^a , P. Spagnolo^a , R. Tenchini^a , G. Tonelli^{a,b} , N. Turini^{a,d} , A. Venturi^a , P.G. Verdini^a

INFN Sezione di Roma^a, Sapienza Università di Roma^b, Roma, Italy

P. Barria^a , C. Basile^{a,b} , M. Campana^{a,b} , F. Cavallari^a , L. Cunqueiro Mendez^{a,b} , D. Del Re^{a,b} , E. Di Marco^a , M. Diemoz^a , F. Errico^{a,b} , E. Longo^{a,b} , P. Meridiani^a , J. Mijuskovic^{a,b} , G. Organtini^{a,b} , F. Pandolfi^a , R. Paramatti^{a,b} , C. Quaranta^{a,b} , S. Rahatlou^{a,b} , C. Rovelli^a , F. Santanastasio^{a,b} , L. Soffi^a

INFN Sezione di Torino^a, Università di Torino^b, Torino, Italy; Università del Piemonte Orientale^c, Novara, Italy

N. Amapane^{a,b} , R. Arcidiacono^{a,c} , S. Argiro^{a,b} , M. Arneodo^{a,c} , N. Bartosik^a , R. Bellan^{a,b} , A. Bellora^{a,b} , C. Biino^a , C. Borca^{a,b} , N. Cartiglia^a , M. Costa^{a,b} , R. Covarelli^{a,b} , N. Demaria^a , L. Finco^a , M. Grippo^{a,b} , B. Kiani^{a,b} , F. Legger^a , F. Luongo^{a,b} , C. Mariotti^a , L. Markovic^{a,b} , S. Maselli^a , A. Mecca^{a,b} , E. Migliore^{a,b} , M. Monteno^a , R. Mulargia^a , M.M. Obertino^{a,b} , G. Ortona^a , L. Pacher^{a,b} , N. Pastrone^a , M. Pelliccioni^a , M. Ruspa^{a,c} , F. Siviero^{a,b} , V. Sola^{a,b} , A. Solano^{a,b} , A. Staiano^a , C. Tarricone^{a,b} , D. Trocino^a , G. Umoret^{a,b}

E. Vlasov^{a,b} , R. White^a 

INFN Sezione di Trieste^a, Università di Trieste^b, Trieste, Italy

S. Belforte^a , V. Candelise^{a,b} , M. Casarsa^a , F. Cossutti^a , K. De Leo^a , G. Della Ricca^{a,b} 

Kyungpook National University, Daegu, Korea

S. Dogra , J. Hong , C. Huh , B. Kim , D.H. Kim , J. Kim, H. Lee, S.W. Lee , C.S. Moon , Y.D. Oh , M.S. Ryu , S. Sekmen , Y.C. Yang 

Department of Mathematics and Physics - GWNU, Gangneung, Korea

M.S. Kim 

Chonnam National University, Institute for Universe and Elementary Particles, Kwangju, Korea

G. Bak , P. Gwak , H. Kim , D.H. Moon 

Hanyang University, Seoul, Korea

E. Asilar , D. Kim , T.J. Kim , J.A. Merlin

Korea University, Seoul, Korea

S. Choi , S. Han, B. Hong , K. Lee, K.S. Lee , S. Lee , J. Park, S.K. Park, J. Yoo 

Kyung Hee University, Department of Physics, Seoul, Korea

J. Goh , S. Yang 

Sejong University, Seoul, Korea

H. S. Kim , Y. Kim, S. Lee

Seoul National University, Seoul, Korea

J. Almond, J.H. Bhyun, J. Choi , W. Jun , J. Kim , S. Ko , H. Kwon , H. Lee , J. Lee , J. Lee , B.H. Oh , S.B. Oh , H. Seo , U.K. Yang, I. Yoon 

University of Seoul, Seoul, Korea

W. Jang , D.Y. Kang, Y. Kang , S. Kim , B. Ko, J.S.H. Lee , Y. Lee , I.C. Park , Y. Roh, I.J. Watson 

Yonsei University, Department of Physics, Seoul, Korea

S. Ha , H.D. Yoo 

Sungkyunkwan University, Suwon, Korea

M. Choi , M.R. Kim , H. Lee, Y. Lee , I. Yu 

College of Engineering and Technology, American University of the Middle East (AUM), Dasman, Kuwait

T. Beyrouty

Riga Technical University, Riga, Latvia

K. Dreimanis , A. Gaile , G. Pikurs, A. Potrebko , M. Seidel , V. Veckalns⁵⁵ 

University of Latvia (LU), Riga, Latvia

N.R. Strautnieks 

Vilnius University, Vilnius, Lithuania

M. Ambrozas , A. Juodagalvis , A. Rinkevicius , G. Tamulaitis 

National Centre for Particle Physics, Universiti Malaya, Kuala Lumpur, Malaysia

N. Bin Norjoharuddeen , I. Yusuff⁵⁶ , Z. Zolkapli

Universidad de Sonora (UNISON), Hermosillo, Mexico

J.F. Benitez , A. Castaneda Hernandez , H.A. Encinas Acosta, L.G. Gallegos Maríñez, M. León Coello , J.A. Murillo Quijada , A. Sehrawat , L. Valencia Palomo 

Centro de Investigacion y de Estudios Avanzados del IPN, Mexico City, Mexico

G. Ayala , H. Castilla-Valdez , H. Crotte Ledesma, E. De La Cruz-Burelo , I. Heredia-De La Cruz⁵⁷ , R. Lopez-Fernandez , C.A. Mondragon Herrera, A. Sánchez Hernández 

Universidad Iberoamericana, Mexico City, Mexico

C. Oropeza Barrera , M. Ramírez García 

Benemerita Universidad Autonoma de Puebla, Puebla, Mexico

I. Bautista , I. Pedraza , H.A. Salazar Ibarguen , C. Uribe Estrada 

University of Montenegro, Podgorica, Montenegro

I. Bubanja , N. Raicevic 

University of Canterbury, Christchurch, New Zealand

P.H. Butler 

National Centre for Physics, Quaid-I-Azam University, Islamabad, Pakistan

A. Ahmad , M.I. Asghar, A. Awais , M.I.M. Awan, H.R. Hoorani , W.A. Khan 

AGH University of Krakow, Faculty of Computer Science, Electronics and Telecommunications, Krakow, Poland

V. Avati, L. Grzanka , M. Malawski 

National Centre for Nuclear Research, Swierk, Poland

H. Bialkowska , M. Bluj , B. Boimska , M. Górski , M. Kazana , M. Szleper , P. Zalewski 

Institute of Experimental Physics, Faculty of Physics, University of Warsaw, Warsaw, Poland

K. Bunkowski , K. Doroba , A. Kalinowski , M. Konecki , J. Krolikowski , A. Muhammad 

Warsaw University of Technology, Warsaw, Poland

K. Pozniak , W. Zabolotny 

Laboratório de Instrumentação e Física Experimental de Partículas, Lisboa, Portugal

M. Araujo , D. Bastos , C. Beirão Da Cruz E Silva , A. Boletti , M. Bozzo , T. Camporesi , G. Da Molin , P. Faccioli , M. Gallinaro , J. Hollar , N. Leonardo , T. Niknejad , A. Petrilli , M. Pisano , J. Seixas , J. Varela , J.W. Wulff

Faculty of Physics, University of Belgrade, Belgrade, Serbia

P. Adzic , P. Milenovic 

VINCA Institute of Nuclear Sciences, University of Belgrade, Belgrade, Serbia

M. Dordevic , J. Milosevic , V. Rekovic

Centro de Investigaciones Energéticas Medioambientales y Tecnológicas (CIEMAT), Madrid, Spain

M. Aguilar-Benitez, J. Alcaraz Maestre , Cristina F. Bedoya , M. Cepeda , M. Cerreda , N. Colino , B. De La Cruz , A. Delgado Peris , A. Escalante Del Valle , D. Fernández Del Val , J.P. Fernández Ramos , J. Flix , M.C. Fouz , O. Gonzalez Lopez , S. Goy Lopez , J.M. Hernandez , M.I. Josa , D. Moran , C. M. Morcillo Perez , Á. Navarro Tobar , C. Perez Dengra , A. Pérez-Calero Yzquierdo , J. Puerta Pelayo 

I. Redondo , D.D. Redondo Ferrero , L. Romero, S. Sánchez Navas , L. Urda Gómez , J. Vazquez Escobar , C. Willmott

Universidad Autónoma de Madrid, Madrid, Spain

J.F. de Trocóniz 

Universidad de Oviedo, Instituto Universitario de Ciencias y Tecnologías Espaciales de Asturias (ICTEA), Oviedo, Spain

B. Alvarez Gonzalez , J. Cuevas , J. Fernandez Menendez , S. Folgueras , I. Gonzalez Caballero , J.R. González Fernández , E. Palencia Cortezon , C. Ramón Álvarez , V. Rodríguez Bouza , A. Soto Rodríguez , A. Trapote , C. Vico Villalba , P. Vischia 

Instituto de Física de Cantabria (IFCA), CSIC-Universidad de Cantabria, Santander, Spain

S. Bhowmik , S. Blanco Fernández , J.A. Brochero Cifuentes , I.J. Cabrillo , A. Calderon , J. Duarte Campderros , M. Fernandez , G. Gomez , C. Lasosa García , C. Martinez Rivero , P. Martinez Ruiz del Arbol , F. Matorras , P. Matorras Cuevas , E. Navarrete Ramos , J. Piedra Gomez , L. Scodellaro , I. Vila , J.M. Vizan Garcia 

University of Colombo, Colombo, Sri Lanka

M.K. Jayananda , B. Kailasapathy⁵⁸ , D.U.J. Sonnadara , D.D.C. Wickramarathna 

University of Ruhuna, Department of Physics, Matara, Sri Lanka

W.G.D. Dharmaratna⁵⁹ , K. Liyanage , N. Perera , N. Wickramage 

CERN, European Organization for Nuclear Research, Geneva, Switzerland

D. Abbaneo , C. Amendola , E. Auffray , G. Auzinger , J. Baechler, D. Barney , A. Bermúdez Martínez , M. Bianco , B. Bilin , A.A. Bin Anuar , A. Bocci , C. Botta , E. Brondolin , C. Caillol , G. Cerminara , N. Chernyavskaya , D. d'Enterria , A. Dabrowski , A. David , A. De Roeck , M.M. Defranchis , M. Deile , M. Dobson , L. Forthomme , G. Franzoni , W. Funk , S. Giani, D. Gigi, K. Gill , F. Glege , L. Gouskos , M. Haranko , J. Hegeman , B. Huber, V. Innocente , T. James , P. Janot , O. Kaluzinska , S. Laurila , P. Lecoq , E. Leutgeb , C. Lourenço , B. Maier , L. Malgeri , M. Mannelli , A.C. Marini , M. Matthewman, F. Meijers , S. Mersi , E. Meschi , V. Milosevic , F. Monti , F. Moortgat , M. Mulders , I. Neutelings , S. Orfanelli, F. Pantaleo , G. Petruciani , A. Pfeiffer , M. Pierini , D. Piparo , H. Qu , D. Rabady , G. Reales Gutiérrez, M. Rovere , H. Sakulin , S. Scarfi , C. Schwick, M. Selvaggi , A. Sharma , K. Shchelina , P. Silva , P. Sphicas⁶⁰ , A.G. Stahl Leiton , A. Steen , S. Summers , D. Treille , P. Tropea , A. Tsirou, D. Walter , J. Wanckzyk⁶¹ , J. Wang, S. Wuchterl , P. Zehetner , P. Zejdl , W.D. Zeuner

Paul Scherrer Institut, Villigen, Switzerland

T. Bevilacqua⁶² , L. Caminada⁶² , A. Ebrahimi , W. Erdmann , R. Horisberger , Q. Ingram , H.C. Kaestli , D. Kotlinski , C. Lange , M. Missiroli⁶² , L. Noehte⁶² , T. Rohe 

ETH Zurich - Institute for Particle Physics and Astrophysics (IPA), Zurich, Switzerland

T.K. Arrestad , K. Androsov⁶¹ , M. Backhaus , A. Calandri , C. Cazzaniga , K. Datta , A. De Cosa , G. Dissertori , M. Dittmar, M. Donegà , F. Eble , M. Galli , K. Gedia , F. Glessgen , C. Grab , D. Hits , W. Lustermann , A.-M. Lyon , R.A. Manzoni , M. Marchegiani , L. Marchese , C. Martin Perez , A. Mascellani⁶¹ , F. Nessi-Tedaldi , F. Pauss , V. Perovic , S. Pigazzini , C. Reissel , T. Reitenspiess , B. Ristic , F. Riti , R. Seidita , J. Steggemann⁶¹ , D. Valsecchi , R. Wallny 

Universität Zürich, Zurich, Switzerland

C. Amsler⁶³ , P. Bärtschi , D. Brzhechko, M.F. Canelli , K. Cormier , J.K. Heikkilä , M. Huwiler , W. Jin , A. Jofrehei , B. Kilminster , S. Leontsinis , S.P. Liechti , A. Macchiolo , P. Meiring , U. Molinatti , A. Reimers , P. Robmann, S. Sanchez Cruz , M. Senger , F. Stäger , Y. Takahashi , R. Tramontano

National Central University, Chung-Li, Taiwan

C. Adloff⁶⁴, D. Bhowmik, C.M. Kuo, W. Lin, P.K. Rout , P.C. Tiwari⁴⁰ , S.S. Yu 

National Taiwan University (NTU), Taipei, Taiwan

L. Ceard, Y. Chao , K.F. Chen , P.s. Chen, Z.g. Chen, A. De Iorio , W.-S. Hou , T.h. Hsu, Y.w. Kao, R. Khurana, G. Kole , Y.y. Li , R.-S. Lu , E. Paganis , X.f. Su , J. Thomas-Wilsker , L.s. Tsai, H.y. Wu, E. Yazgan

High Energy Physics Research Unit, Department of Physics, Faculty of Science, Chulalongkorn University, Bangkok, Thailand

C. Asawatangtrakuldee , N. Srimanobhas , V. Wachirapusanand 

Çukurova University, Physics Department, Science and Art Faculty, Adana, Turkey

D. Agyel , F. Boran , Z.S. Demiroglu , F. Dolek , I. Dumanoglu⁶⁵ , E. Eskut , Y. Guler⁶⁶ , E. Gurpinar Guler⁶⁶ , C. Isik , O. Kara, A. Kayis Topaksu , U. Kiminsu , G. Onengut , K. Ozdemir⁶⁷ , A. Polatoz , B. Tali⁶⁸ , U.G. Tok , S. Turkcapar , E. Uslan , I.S. Zorbakir

Middle East Technical University, Physics Department, Ankara, Turkey

M. Yalvac⁶⁹ 

Bogazici University, Istanbul, Turkey

B. Akgun , I.O. Atakisi , E. Gülmez , M. Kaya⁷⁰ , O. Kaya⁷¹ , S. Tekten⁷² 

Istanbul Technical University, Istanbul, Turkey

A. Cakir , K. Cankocak^{65,73} , Y. Komurcu , S. Sen⁷⁴ 

Istanbul University, Istanbul, Turkey

O. Aydilek²⁵ , S. Cerci⁶⁸ , V. Epshteyn , B. Hacisahinoglu , I. Hos⁷⁵ , B. Kaynak , S. Ozkorucuklu , O. Potok , H. Sert , C. Simsek , C. Zorbilmez

Yildiz Technical University, Istanbul, Turkey

B. Isildak⁷⁶ , D. Sunar Cerci⁶⁸ 

Institute for Scintillation Materials of National Academy of Science of Ukraine, Kharkiv, Ukraine

A. Boyaryntsev , B. Grynyov 

National Science Centre, Kharkiv Institute of Physics and Technology, Kharkiv, Ukraine

L. Levchuk 

University of Bristol, Bristol, United Kingdom

D. Anthony , J.J. Brooke , A. Bundock , F. Bury , E. Clement , D. Cussans , H. Flacher , M. Glowacki, J. Goldstein , H.F. Heath , L. Kreczko , S. Paramesvaran , L. Robertshaw, S. Seif El Nasr-Storey, V.J. Smith , N. Stylianou⁷⁷ , K. Walkingshaw Pass

Rutherford Appleton Laboratory, Didcot, United Kingdom

A.H. Ball, K.W. Bell , A. Belyaev⁷⁸ , C. Brew , R.M. Brown , D.J.A. Cockerill , C. Cooke , K.V. Ellis, K. Harder , S. Harper , M.-L. Holmberg⁷⁹ , J. Linacre , K. Manolopoulos, D.M. Newbold , E. Olaiya, D. Petyt , T. Reis , A.R. Sahasransu , G. Salvi , T. Schuh, C.H. Shepherd-Themistocleous , I.R. Tomalin , T. Williams

Imperial College, London, United Kingdom

R. Bainbridge , P. Bloch , C.E. Brown , O. Buchmuller, V. Cacchio, C.A. Carrillo Montoya , G.S. Chahal⁸⁰ , D. Colling , J.S. Dancu, I. Das , P. Dauncey , G. Davies , J. Davies, M. Della Negra , S. Fayer, G. Fedi , G. Hall , M.H. Hassanshahi , A. Howard, G. Iles , M. Knight , J. Langford , J. León Holgado , L. Lyons , A.-M. Magnan , S. Malik, M. Mieskolainen , J. Nash⁸¹ , M. Pesaresi , B.C. Radburn-Smith , A. Richards, A. Rose , K. Savva , C. Seez , R. Shukla , A. Tapper , K. Uchida , G.P. Uttley , L.H. Vage, T. Virdee³² , M. Vojinovic , N. Wardle , D. Winterbottom

Brunel University, Uxbridge, United Kingdom

K. Coldham, J.E. Cole , A. Khan, P. Kyberd , I.D. Reid 

Baylor University, Waco, Texas, USA

S. Abdullin , A. Brinkerhoff , B. Caraway , E. Collins , J. Dittmann , K. Hatakeyama , J. Hiltbrand , B. McMaster , M. Saunders , S. Sawant , C. Sutantawibul , J. Wilson

Catholic University of America, Washington, DC, USA

R. Bartek , A. Dominguez , C. Huerta Escamilla, A.E. Simsek , R. Uniyal , A.M. Vargas Hernandez 

The University of Alabama, Tuscaloosa, Alabama, USA

B. Bam , R. Chudasama , S.I. Cooper , S.V. Gleyzer , C.U. Perez , P. Rumerio⁸² , E. Usai , R. Yi 

Boston University, Boston, Massachusetts, USA

A. Akpinar , D. Arcaro , C. Cosby , Z. Demiragli , C. Erice , C. Fangmeier , C. Fernandez Madrazo , E. Fontanesi , D. Gastler , F. Golf , S. Jeon , I. Reed , J. Rohlf , K. Salyer , D. Sperka , D. Spitzbart , I. Suarez , A. Tsatsos , S. Yuan , A.G. Zecchinelli

Brown University, Providence, Rhode Island, USA

G. Benelli , X. Coubez²⁷ , D. Cutts , M. Hadley , U. Heintz , J.M. Hogan⁸³ , T. Kwon , G. Landsberg , K.T. Lau , D. Li , J. Luo , S. Mondal , M. Narain[†] , N. Pervan , S. Sagir⁸⁴ , F. Simpson , M. Stamenkovic , X. Yan , W. Zhang

University of California, Davis, Davis, California, USA

S. Abbott , J. Bonilla , C. Brainerd , R. Breedon , H. Cai , M. Calderon De La Barca Sanchez , M. Chertok , M. Citron , J. Conway , P.T. Cox , R. Erbacher , F. Jensen , O. Kukral , G. Mocellin , M. Mulhearn , D. Pellett , W. Wei , Y. Yao , F. Zhang

University of California, Los Angeles, California, USA

M. Bachtis , R. Cousins , A. Datta , G. Flores Avila , J. Hauser , M. Ignatenko , M.A. Iqbal , T. Lam , E. Manca , A. Nunez Del Prado, D. Saltzberg , V. Valuev

University of California, Riverside, Riverside, California, USA

R. Clare , J.W. Gary , M. Gordon, G. Hanson , W. Si , S. Wimpenny[†] 

University of California, San Diego, La Jolla, California, USA

J.G. Branson , S. Cittolin , S. Cooperstein , D. Diaz , J. Duarte , L. Giannini , J. Guiang , R. Kansal , V. Krutelyov , R. Lee , J. Letts , M. Masciovecchio , F. Mokhtar , S. Mukherjee , M. Pieri , M. Quinnan , B.V. Sathia Narayanan , V. Sharma , M. Tadel , E. Vourliotis , F. Würthwein , Y. Xiang , A. Yagil

University of California, Santa Barbara - Department of Physics, Santa Barbara, California,

USA

A. Barzdukas [ID](#), L. Brennan [ID](#), C. Campagnari [ID](#), J. Incandela [ID](#), J. Kim [ID](#), A.J. Li [ID](#), P. Masterson [ID](#), H. Mei [ID](#), J. Richman [ID](#), U. Sarica [ID](#), R. Schmitz [ID](#), F. Setti [ID](#), J. Sheplock [ID](#), D. Stuart [ID](#), T.Á. Vámi [ID](#), S. Wang [ID](#)

California Institute of Technology, Pasadena, California, USA

A. Bornheim [ID](#), O. Cerri, A. Latorre, J. Mao [ID](#), H.B. Newman [ID](#), M. Spiropulu [ID](#), J.R. Vlimant [ID](#), C. Wang [ID](#), S. Xie [ID](#), R.Y. Zhu [ID](#)

Carnegie Mellon University, Pittsburgh, Pennsylvania, USA

J. Alison [ID](#), S. An [ID](#), M.B. Andrews [ID](#), P. Bryant [ID](#), M. Cremonesi, V. Dutta [ID](#), T. Ferguson [ID](#), A. Harilal [ID](#), C. Liu [ID](#), T. Mudholkar [ID](#), S. Murthy [ID](#), P. Palit [ID](#), M. Paulini [ID](#), A. Roberts [ID](#), A. Sanchez [ID](#), W. Terrill [ID](#)

University of Colorado Boulder, Boulder, Colorado, USA

J.P. Cumalat [ID](#), W.T. Ford [ID](#), A. Hart [ID](#), A. Hassani [ID](#), G. Karathanasis [ID](#), E. MacDonald, N. Manganelli [ID](#), A. Perloff [ID](#), C. Savard [ID](#), N. Schonbeck [ID](#), K. Stenson [ID](#), K.A. Ulmer [ID](#), S.R. Wagner [ID](#), N. Zipper [ID](#)

Cornell University, Ithaca, New York, USA

J. Alexander [ID](#), S. Bright-Thonney [ID](#), X. Chen [ID](#), D.J. Cranshaw [ID](#), J. Fan [ID](#), X. Fan [ID](#), D. Gadkari [ID](#), S. Hogan [ID](#), P. Kotamnives, J. Monroy [ID](#), M. Oshiro [ID](#), J.R. Patterson [ID](#), J. Reichert [ID](#), M. Reid [ID](#), A. Ryd [ID](#), J. Thom [ID](#), P. Wittich [ID](#), R. Zou [ID](#)

Fermi National Accelerator Laboratory, Batavia, Illinois, USA

M. Albrow [ID](#), M. Alyari [ID](#), O. Amram [ID](#), G. Apollinari [ID](#), A. Apresyan [ID](#), L.A.T. Bauerdick [ID](#), D. Berry [ID](#), J. Berryhill [ID](#), P.C. Bhat [ID](#), K. Burkett [ID](#), J.N. Butler [ID](#), A. Canepa [ID](#), G.B. Cerati [ID](#), H.W.K. Cheung [ID](#), F. Chlebana [ID](#), G. Cummings [ID](#), J. Dickinson [ID](#), I. Dutta [ID](#), V.D. Elvira [ID](#), Y. Feng [ID](#), J. Freeman [ID](#), A. Gandrakota [ID](#), Z. Gecse [ID](#), L. Gray [ID](#), D. Green, A. Grummer [ID](#), S. Grünendahl [ID](#), D. Guerrero [ID](#), O. Gutsche [ID](#), R.M. Harris [ID](#), R. Heller [ID](#), T.C. Herwig [ID](#), J. Hirschauer [ID](#), L. Horyn [ID](#), B. Jayatilaka [ID](#), S. Jindariani [ID](#), M. Johnson [ID](#), U. Joshi [ID](#), T. Klijnsma [ID](#), B. Klima [ID](#), K.H.M. Kwok [ID](#), S. Lammel [ID](#), D. Lincoln [ID](#), R. Lipton [ID](#), T. Liu [ID](#), C. Madrid [ID](#), K. Maeshima [ID](#), C. Mantilla [ID](#), D. Mason [ID](#), P. McBride [ID](#), P. Merkel [ID](#), S. Mrenna [ID](#), S. Nahm [ID](#), J. Ngadiuba [ID](#), D. Noonan [ID](#), V. Papadimitriou [ID](#), N. Pastika [ID](#), K. Pedro [ID](#), C. Pena⁸⁵ [ID](#), F. Ravera [ID](#), A. Reinsvold Hall⁸⁶ [ID](#), L. Ristori [ID](#), E. Sexton-Kennedy [ID](#), N. Smith [ID](#), A. Soha [ID](#), L. Spiegel [ID](#), S. Stoynev [ID](#), J. Strait [ID](#), L. Taylor [ID](#), S. Tkaczyk [ID](#), N.V. Tran [ID](#), L. Uplegger [ID](#), E.W. Vaandering [ID](#), A. Whitbeck [ID](#), I. Zoi [ID](#)

University of Florida, Gainesville, Florida, USA

C. Aruta [ID](#), P. Avery [ID](#), D. Bourilkov [ID](#), L. Cadamuro [ID](#), P. Chang [ID](#), V. Cherepanov [ID](#), R.D. Field, E. Koenig [ID](#), M. Kolosova [ID](#), J. Konigsberg [ID](#), A. Korytov [ID](#), K. Matchev [ID](#), N. Menendez [ID](#), G. Mitselmakher [ID](#), K. Mohrman [ID](#), A. Muthirakalayil Madhu [ID](#), N. Rawal [ID](#), D. Rosenzweig [ID](#), S. Rosenzweig [ID](#), J. Wang [ID](#)

Florida State University, Tallahassee, Florida, USA

T. Adams [ID](#), A. Al Kadhim [ID](#), A. Askew [ID](#), S. Bower [ID](#), R. Habibullah [ID](#), V. Hagopian [ID](#), R. Hashmi [ID](#), R.S. Kim [ID](#), S. Kim [ID](#), T. Kolberg [ID](#), G. Martinez, H. Prosper [ID](#), P.R. Prova, M. Wulansatiti [ID](#), R. Yohay [ID](#), J. Zhang

Florida Institute of Technology, Melbourne, Florida, USA

B. Alsufyani, M.M. Baarmand [ID](#), S. Butalla [ID](#), S. Das [ID](#), T. Elkafrawy²⁰ [ID](#), M. Hohlmann [ID](#), R. Kumar Verma [ID](#), M. Rahmani, E. Yanes

University of Illinois Chicago, Chicago, USA, Chicago, USA

M.R. Adams [ID](#), A. Baty [ID](#), C. Bennett, R. Cavanaugh [ID](#), R. Escobar Franco [ID](#), O. Evdokimov [ID](#), C.E. Gerber [ID](#), D.J. Hofman [ID](#), J.h. Lee [ID](#), D. S. Lemos [ID](#), A.H. Merrit [ID](#), C. Mills [ID](#), S. Nanda [ID](#), G. Oh [ID](#), B. Ozek [ID](#), D. Pilipovic [ID](#), R. Pradhan [ID](#), T. Roy [ID](#), S. Rudrabhatla [ID](#), M.B. Tonjes [ID](#), N. Varelas [ID](#), Z. Ye [ID](#), J. Yoo [ID](#)

The University of Iowa, Iowa City, Iowa, USA

M. Alhusseini [ID](#), D. Blend, K. Dilsiz⁸⁷ [ID](#), L. Emediato [ID](#), G. Karaman [ID](#), O.K. Köseyan [ID](#), J.-P. Merlo, A. Mestvirishvili⁸⁸ [ID](#), J. Nachtman [ID](#), O. Neogi, H. Ogul⁸⁹ [ID](#), Y. Onel [ID](#), A. Penzo [ID](#), C. Snyder, E. Tiras⁹⁰ [ID](#)

Johns Hopkins University, Baltimore, Maryland, USA

B. Blumenfeld [ID](#), L. Corcodilos [ID](#), J. Davis [ID](#), A.V. Gritsan [ID](#), L. Kang [ID](#), S. Kyriacou [ID](#), P. Maksimovic [ID](#), M. Roguljic [ID](#), J. Roskes [ID](#), S. Sekhar [ID](#), M. Swartz [ID](#)

The University of Kansas, Lawrence, Kansas, USA

A. Abreu [ID](#), L.F. Alcerro Alcerro [ID](#), J. Anguiano [ID](#), P. Baringer [ID](#), A. Bean [ID](#), Z. Flowers [ID](#), D. Grove [ID](#), J. King [ID](#), G. Krintiras [ID](#), M. Lazarovits [ID](#), C. Le Mahieu [ID](#), J. Marquez [ID](#), N. Minafra [ID](#), M. Murray [ID](#), M. Nickel [ID](#), M. Pitt [ID](#), S. Popescu⁹¹ [ID](#), C. Rogan [ID](#), C. Royon [ID](#), R. Salvatico [ID](#), S. Sanders [ID](#), C. Smith [ID](#), Q. Wang [ID](#), G. Wilson [ID](#)

Kansas State University, Manhattan, Kansas, USA

B. Allmond [ID](#), A. Ivanov [ID](#), K. Kaadze [ID](#), A. Kalogeropoulos [ID](#), D. Kim, Y. Maravin [ID](#), J. Natoli [ID](#), D. Roy [ID](#), G. Sorrentino [ID](#)

Lawrence Livermore National Laboratory, Livermore, California, USA

F. Rebassoo [ID](#), D. Wright [ID](#)

University of Maryland, College Park, Maryland, USA

A. Baden [ID](#), A. Belloni [ID](#), Y.M. Chen [ID](#), S.C. Eno [ID](#), N.J. Hadley [ID](#), S. Jabeen [ID](#), R.G. Kellogg [ID](#), T. Koeth [ID](#), Y. Lai [ID](#), S. Lascio [ID](#), A.C. Mignerey [ID](#), S. Nabili [ID](#), C. Palmer [ID](#), C. Papageorgakis [ID](#), M.M. Paranjpe, L. Wang [ID](#)

Massachusetts Institute of Technology, Cambridge, Massachusetts, USA

J. Bendavid [ID](#), I.A. Cali [ID](#), M. D'Alfonso [ID](#), J. Eysermans [ID](#), C. Freer [ID](#), G. Gomez-Ceballos [ID](#), M. Goncharov, G. Grossos, P. Harris, D. Hoang, D. Kovalskyi [ID](#), J. Krupa [ID](#), L. Lavezzi [ID](#), Y.-J. Lee [ID](#), K. Long [ID](#), A. Novak [ID](#), C. Paus [ID](#), D. Rankin [ID](#), C. Roland [ID](#), G. Roland [ID](#), S. Rothman [ID](#), G.S.F. Stephans [ID](#), Z. Wang [ID](#), B. Wyslouch [ID](#), T. J. Yang [ID](#)

University of Minnesota, Minneapolis, Minnesota, USA

B. Crossman [ID](#), B.M. Joshi [ID](#), C. Kapsiak [ID](#), M. Krohn [ID](#), D. Mahon [ID](#), J. Mans [ID](#), B. Marzocchi [ID](#), S. Pandey [ID](#), M. Revering [ID](#), R. Rusack [ID](#), R. Saradhy [ID](#), N. Schroeder [ID](#), N. Strobbe [ID](#), M.A. Wadud [ID](#)

University of Mississippi, Oxford, Mississippi, USA

L.M. Cremaldi [ID](#)

University of Nebraska-Lincoln, Lincoln, Nebraska, USA

K. Bloom [ID](#), D.R. Claes [ID](#), G. Haza [ID](#), J. Hossain [ID](#), C. Joo [ID](#), I. Kravchenko [ID](#), J.E. Siado [ID](#), W. Tabb [ID](#), A. Vagnerini [ID](#), A. Wightman [ID](#), F. Yan [ID](#), D. Yu [ID](#)

State University of New York at Buffalo, Buffalo, New York, USA

H. Bandyopadhyay [ID](#), L. Hay [ID](#), I. Iashvili [ID](#), A. Kharchilava [ID](#), M. Morris [ID](#), D. Nguyen [ID](#), S. Rappoccio [ID](#), H. Rejeb Sfar, A. Williams [ID](#)

Northeastern University, Boston, Massachusetts, USA

G. Alverson [id](#), E. Barberis [id](#), J. Dervan, Y. Haddad [id](#), Y. Han [id](#), A. Krishna [id](#), J. Li [id](#), M. Lu [id](#), G. Madigan [id](#), R. McCarthy [id](#), D.M. Morse [id](#), V. Nguyen [id](#), T. Orimoto [id](#), A. Parker [id](#), L. Skinnari [id](#), B. Wang [id](#), D. Wood [id](#)

Northwestern University, Evanston, Illinois, USA

S. Bhattacharya [id](#), J. Bueghly, Z. Chen [id](#), S. Dittmer [id](#), K.A. Hahn [id](#), Y. Liu [id](#), Y. Miao [id](#), D.G. Monk [id](#), M.H. Schmitt [id](#), A. Taliercio [id](#), M. Velasco

University of Notre Dame, Notre Dame, Indiana, USA

G. Agarwal [id](#), R. Band [id](#), R. Bucci, S. Castells [id](#), A. Das [id](#), R. Goldouzian [id](#), M. Hildreth [id](#), K.W. Ho [id](#), K. Hurtado Anampa [id](#), T. Ivanov [id](#), C. Jessop [id](#), K. Lannon [id](#), J. Lawrence [id](#), N. Loukas [id](#), L. Lutton [id](#), J. Mariano, N. Marinelli, I. Mcalister, T. McCauley [id](#), C. Mcgrady [id](#), C. Moore [id](#), Y. Musienko¹⁶ [id](#), H. Nelson [id](#), M. Osherson [id](#), A. Piccinelli [id](#), R. Ruchti [id](#), A. Townsend [id](#), Y. Wan, M. Wayne [id](#), H. Yockey, M. Zarucki [id](#), L. Zygalas [id](#)

The Ohio State University, Columbus, Ohio, USA

A. Basnet [id](#), B. Bylsma, M. Carrigan [id](#), L.S. Durkin [id](#), C. Hill [id](#), M. Joyce [id](#), M. Nunez Ornelas [id](#), K. Wei, B.L. Winer [id](#), B. R. Yates [id](#)

Princeton University, Princeton, New Jersey, USA

F.M. Addesa [id](#), H. Bouchamaoui [id](#), P. Das [id](#), G. Dezoort [id](#), P. Elmer [id](#), A. Frankenthal [id](#), B. Greenberg [id](#), N. Haubrich [id](#), G. Kopp [id](#), S. Kwan [id](#), D. Lange [id](#), A. Loeliger [id](#), D. Marlow [id](#), I. Ojalvo [id](#), J. Olsen [id](#), A. Shevelev [id](#), D. Stickland [id](#), C. Tully [id](#)

University of Puerto Rico, Mayaguez, Puerto Rico, USA

S. Malik [id](#)

Purdue University, West Lafayette, Indiana, USA

A.S. Bakshi [id](#), V.E. Barnes [id](#), S. Chandra [id](#), R. Chawla [id](#), A. Gu [id](#), L. Gutay, M. Jones [id](#), A.W. Jung [id](#), D. Kondratyev [id](#), A.M. Koshy, M. Liu [id](#), G. Negro [id](#), N. Neumeister [id](#), G. Paspalaki [id](#), S. Piperov [id](#), V. Scheurer, J.F. Schulte [id](#), M. Stojanovic [id](#), J. Thieman [id](#), A. K. Virdi [id](#), F. Wang [id](#), W. Xie [id](#)

Purdue University Northwest, Hammond, Indiana, USA

J. Dolen [id](#), N. Parashar [id](#), A. Pathak [id](#)

Rice University, Houston, Texas, USA

D. Acosta [id](#), T. Carnahan [id](#), K.M. Ecklund [id](#), P.J. Fernández Manteca [id](#), S. Freed, P. Gardner, F.J.M. Geurts [id](#), W. Li [id](#), O. Miguel Colin [id](#), B.P. Padley [id](#), R. Redjimi, J. Rotter [id](#), E. Yigitbasi [id](#), Y. Zhang [id](#)

University of Rochester, Rochester, New York, USA

A. Bodek [id](#), P. de Barbaro [id](#), R. Demina [id](#), J.L. Dulemba [id](#), A. Garcia-Bellido [id](#), O. Hindrichs [id](#), A. Khukhunaishvili [id](#), N. Parmar, P. Parygin⁹² [id](#), E. Popova⁹² [id](#), R. Taus [id](#)

The Rockefeller University, New York, New York, USA

K. Goulianatos [id](#)

Rutgers, The State University of New Jersey, Piscataway, New Jersey, USA

B. Chiarito, J.P. Chou [id](#), S.V. Clark [id](#), Y. Gershten [id](#), E. Halkiadakis [id](#), M. Heindl [id](#), C. Houghton [id](#), D. Jaroslawski [id](#), O. Karacheban³⁰ [id](#), I. Laflotte [id](#), A. Lath [id](#), R. Montalvo, K. Nash, H. Routray [id](#), S. Salur [id](#), S. Schnetzer, S. Somalwar [id](#), R. Stone [id](#), S.A. Thayil [id](#), S. Thomas, J. Vora [id](#), H. Wang [id](#)

University of Tennessee, Knoxville, Tennessee, USA

H. Acharya, D. Ally [ID](#), A.G. Delannoy [ID](#), S. Fiorendi [ID](#), S. Higginbotham [ID](#), T. Holmes [ID](#), A.R. Kanuganti [ID](#), N. Karunaratnha [ID](#), L. Lee [ID](#), E. Nibigira [ID](#), S. Spanier [ID](#)

Texas A&M University, College Station, Texas, USA

D. Aebi [ID](#), M. Ahmad [ID](#), O. Bouhali⁹³ [ID](#), R. Eusebi [ID](#), J. Gilmore [ID](#), T. Huang [ID](#), T. Kamon⁹⁴ [ID](#), H. Kim [ID](#), S. Luo [ID](#), R. Mueller [ID](#), D. Overton [ID](#), D. Rathjens [ID](#), A. Safonov [ID](#)

Texas Tech University, Lubbock, Texas, USA

N. Akchurin [ID](#), J. Damgov [ID](#), V. Hegde [ID](#), A. Hussain [ID](#), Y. Kazhykarim, K. Lamichhane [ID](#), S.W. Lee [ID](#), A. Mankel [ID](#), T. Peltola [ID](#), I. Volobouev [ID](#)

Vanderbilt University, Nashville, Tennessee, USA

E. Appelt [ID](#), Y. Chen [ID](#), S. Greene, A. Gurrola [ID](#), W. Johns [ID](#), R. Kunawalkam Elayavalli [ID](#), A. Melo [ID](#), F. Romeo [ID](#), P. Sheldon [ID](#), S. Tuo [ID](#), J. Velkovska [ID](#), J. Viinikainen [ID](#)

University of Virginia, Charlottesville, Virginia, USA

B. Cardwell [ID](#), B. Cox [ID](#), J. Hakala [ID](#), R. Hirosky [ID](#), A. Ledovskoy [ID](#), C. Neu [ID](#), C.E. Perez Lara [ID](#)

Wayne State University, Detroit, Michigan, USA

P.E. Karchin [ID](#)

University of Wisconsin - Madison, Madison, Wisconsin, USA

A. Aravind, S. Banerjee [ID](#), K. Black [ID](#), T. Bose [ID](#), S. Dasu [ID](#), I. De Bruyn [ID](#), P. Everaerts [ID](#), C. Galloni, H. He [ID](#), M. Herndon [ID](#), A. Herve [ID](#), C.K. Koraka [ID](#), A. Lanaro, R. Loveless [ID](#), J. Madhusudanan Sreekala [ID](#), A. Mallampalli [ID](#), A. Mohammadi [ID](#), S. Mondal, G. Parida [ID](#), L. Pétré [ID](#), D. Pinna, A. Savin, V. Shang [ID](#), V. Sharma [ID](#), W.H. Smith [ID](#), D. Teague, H.F. Tsoi [ID](#), W. Vetens [ID](#), A. Warden [ID](#)

Authors affiliated with an institute or an international laboratory covered by a cooperation agreement with CERN

S. Afanasiev [ID](#), D. Budkouski [ID](#), I. Golutvin [ID](#), I. Gorbunov [ID](#), V. Karjavine [ID](#), V. Korenkov [ID](#), A. Lanev [ID](#), A. Malakhov [ID](#), V. Matveev⁹⁵ [ID](#), V. Palichik [ID](#), V. Perelygin [ID](#), M. Savina [ID](#), V. Shalaev [ID](#), S. Shmatov [ID](#), S. Shulha [ID](#), V. Smirnov [ID](#), O. Teryaev [ID](#), N. Voytishin [ID](#), B.S. Yuldashev⁹⁶, A. Zarubin [ID](#), I. Zhizhin [ID](#), G. Gavrilov [ID](#), V. Golovtcov [ID](#), Y. Ivanov [ID](#), V. Kim⁹⁵ [ID](#), P. Levchenko⁹⁷ [ID](#), V. Murzin [ID](#), V. Oreshkin [ID](#), D. Sosnov [ID](#), V. Sulimov [ID](#), L. Uvarov [ID](#), A. Vorobyev[†], Yu. Andreev [ID](#), A. Dermenev [ID](#), S. Gninenko [ID](#), N. Golubev [ID](#), A. Karneyeu [ID](#), D. Kirpichnikov [ID](#), M. Kirsanov [ID](#), N. Krasnikov [ID](#), I. Tlisova [ID](#), A. Toropin [ID](#), T. Aushev [ID](#), V. Gavrilov [ID](#), N. Lychkovskaya [ID](#), A. Nikitenko^{98,99} [ID](#), V. Popov [ID](#), A. Zhokin [ID](#), R. Chistov⁹⁵ [ID](#), M. Danilov⁹⁵ [ID](#), S. Polikarpov⁹⁵ [ID](#), V. Andreev [ID](#), M. Azarkin [ID](#), M. Kirakosyan, A. Terkulov [ID](#), A. Belyaev [ID](#), E. Boos [ID](#), V. Bunichev [ID](#), M. Dubinin⁸⁵ [ID](#), L. Dudko [ID](#), A. Gribushin [ID](#), V. Klyukhin [ID](#), O. Kodolova⁹⁹ [ID](#), S. Obraztsov [ID](#), M. Perfilov, S. Petrushanko [ID](#), V. Savrin [ID](#), G. Vorotnikov [ID](#), V. Blinov⁹⁵, T. Dimova⁹⁵ [ID](#), A. Kozyrev⁹⁵ [ID](#), O. Radchenko⁹⁵ [ID](#), Y. Skovpen⁹⁵ [ID](#), V. Kachanov [ID](#), D. Konstantinov [ID](#), S. Slabospitskii [ID](#), A. Uzunian [ID](#), A. Babaev [ID](#), V. Borshch [ID](#), D. Druzhkin¹⁰⁰ [ID](#), E. Tcherniaev [ID](#)

Authors affiliated with an institute formerly covered by a cooperation agreement with CERN
V. Chekhovsky, V. Makarenko [ID](#)

†: Deceased

¹Also at Yerevan State University, Yerevan, Armenia

²Also at TU Wien, Vienna, Austria

³Also at Institute of Basic and Applied Sciences, Faculty of Engineering, Arab Academy for

Science, Technology and Maritime Transport, Alexandria, Egypt

⁴Also at Ghent University, Ghent, Belgium

⁵Also at Universidade Estadual de Campinas, Campinas, Brazil

⁶Also at Federal University of Rio Grande do Sul, Porto Alegre, Brazil

⁷Also at UFMS, Nova Andradina, Brazil

⁸Also at Nanjing Normal University, Nanjing, China

⁹Now at The University of Iowa, Iowa City, Iowa, USA

¹⁰Also at University of Chinese Academy of Sciences, Beijing, China

¹¹Also at China Center of Advanced Science and Technology, Beijing, China

¹²Also at University of Chinese Academy of Sciences, Beijing, China

¹³Also at China Spallation Neutron Source, Guangdong, China

¹⁴Now at Henan Normal University, Xinxiang, China

¹⁵Also at Université Libre de Bruxelles, Bruxelles, Belgium

¹⁶Also at an institute or an international laboratory covered by a cooperation agreement with CERN

¹⁷Also at Helwan University, Cairo, Egypt

¹⁸Now at Zewail City of Science and Technology, Zewail, Egypt

¹⁹Also at British University in Egypt, Cairo, Egypt

²⁰Now at Ain Shams University, Cairo, Egypt

²¹Also at Purdue University, West Lafayette, Indiana, USA

²²Also at Université de Haute Alsace, Mulhouse, France

²³Also at İstinye University, Istanbul, Turkey

²⁴Also at The University of the State of Amazonas, Manaus, Brazil

²⁵Also at Erzincan Binali Yıldırım University, Erzincan, Turkey

²⁶Also at University of Hamburg, Hamburg, Germany

²⁷Also at RWTH Aachen University, III. Physikalisches Institut A, Aachen, Germany

²⁸Also at Isfahan University of Technology, Isfahan, Iran

²⁹Also at Bergische University Wuppertal (B UW), Wuppertal, Germany

³⁰Also at Brandenburg University of Technology, Cottbus, Germany

³¹Also at Forschungszentrum Jülich, Juelich, Germany

³²Also at CERN, European Organization for Nuclear Research, Geneva, Switzerland

³³Also at Institute of Physics, University of Debrecen, Debrecen, Hungary

³⁴Also at Institute of Nuclear Research ATOMKI, Debrecen, Hungary

³⁵Now at Universitatea Babes-Bolyai - Facultatea de Fizica, Cluj-Napoca, Romania

³⁶Also at Physics Department, Faculty of Science, Assiut University, Assiut, Egypt

³⁷Also at HUN-REN Wigner Research Centre for Physics, Budapest, Hungary

³⁸Also at Punjab Agricultural University, Ludhiana, India

³⁹Also at University of Visva-Bharati, Santiniketan, India

⁴⁰Also at Indian Institute of Science (IISc), Bangalore, India

⁴¹Also at Birla Institute of Technology, Mesra, Mesra, India

⁴²Also at IIT Bhubaneswar, Bhubaneswar, India

⁴³Also at Institute of Physics, Bhubaneswar, India

⁴⁴Also at University of Hyderabad, Hyderabad, India

⁴⁵Also at Deutsches Elektronen-Synchrotron, Hamburg, Germany

⁴⁶Also at Department of Physics, Isfahan University of Technology, Isfahan, Iran

⁴⁷Also at Sharif University of Technology, Tehran, Iran

⁴⁸Also at Department of Physics, University of Science and Technology of Mazandaran, Behshahr, Iran

⁴⁹Also at Italian National Agency for New Technologies, Energy and Sustainable Economic

Development, Bologna, Italy

⁵⁰Also at Centro Siciliano di Fisica Nucleare e di Struttura Della Materia, Catania, Italy

⁵¹Also at Università degli Studi Guglielmo Marconi, Roma, Italy

⁵²Also at Scuola Superiore Meridionale, Università di Napoli 'Federico II', Napoli, Italy

⁵³Also at Fermi National Accelerator Laboratory, Batavia, Illinois, USA

⁵⁴Also at Consiglio Nazionale delle Ricerche - Istituto Officina dei Materiali, Perugia, Italy

⁵⁵Also at Riga Technical University, Riga, Latvia

⁵⁶Also at Department of Applied Physics, Faculty of Science and Technology, Universiti Kebangsaan Malaysia, Bangi, Malaysia

⁵⁷Also at Consejo Nacional de Ciencia y Tecnología, Mexico City, Mexico

⁵⁸Also at Trincomalee Campus, Eastern University, Sri Lanka, Nilaveli, Sri Lanka

⁵⁹Also at Saegis Campus, Nugegoda, Sri Lanka

⁶⁰Also at National and Kapodistrian University of Athens, Athens, Greece

⁶¹Also at Ecole Polytechnique Fédérale Lausanne, Lausanne, Switzerland

⁶²Also at Universität Zürich, Zurich, Switzerland

⁶³Also at Stefan Meyer Institute for Subatomic Physics, Vienna, Austria

⁶⁴Also at Laboratoire d'Annecy-le-Vieux de Physique des Particules, IN2P3-CNRS, Annecy-le-Vieux, France

⁶⁵Also at Near East University, Research Center of Experimental Health Science, Mersin, Turkey

⁶⁶Also at Konya Technical University, Konya, Turkey

⁶⁷Also at Izmir Bakircay University, Izmir, Turkey

⁶⁸Also at Adiyaman University, Adiyaman, Turkey

⁶⁹Also at Bozok Universitetesi Rektörlüğü, Yozgat, Turkey

⁷⁰Also at Marmara University, Istanbul, Turkey

⁷¹Also at Milli Savunma University, Istanbul, Turkey

⁷²Also at Kafkas University, Kars, Turkey

⁷³Now at Istanbul Okan University, Istanbul, Turkey

⁷⁴Also at Hacettepe University, Ankara, Turkey

⁷⁵Also at Istanbul University - Cerrahpasa, Faculty of Engineering, Istanbul, Turkey

⁷⁶Also at Yildiz Technical University, Istanbul, Turkey

⁷⁷Also at Vrije Universiteit Brussel, Brussel, Belgium

⁷⁸Also at School of Physics and Astronomy, University of Southampton, Southampton, United Kingdom

⁷⁹Also at University of Bristol, Bristol, United Kingdom

⁸⁰Also at IPPP Durham University, Durham, United Kingdom

⁸¹Also at Monash University, Faculty of Science, Clayton, Australia

⁸²Also at Università di Torino, Torino, Italy

⁸³Also at Bethel University, St. Paul, Minnesota, USA

⁸⁴Also at Karamanoğlu Mehmetbey University, Karaman, Turkey

⁸⁵Also at California Institute of Technology, Pasadena, California, USA

⁸⁶Also at United States Naval Academy, Annapolis, Maryland, USA

⁸⁷Also at Bingol University, Bingol, Turkey

⁸⁸Also at Georgian Technical University, Tbilisi, Georgia

⁸⁹Also at Sinop University, Sinop, Turkey

⁹⁰Also at Erciyes University, Kayseri, Turkey

⁹¹Also at Horia Hulubei National Institute of Physics and Nuclear Engineering (IFIN-HH), Bucharest, Romania

⁹²Now at another institute or international laboratory covered by a cooperation agreement

with CERN

⁹³Also at Texas A&M University at Qatar, Doha, Qatar

⁹⁴Also at Kyungpook National University, Daegu, Korea

⁹⁵Also at another institute or international laboratory covered by a cooperation agreement with CERN

⁹⁶Also at Institute of Nuclear Physics of the Uzbekistan Academy of Sciences, Tashkent, Uzbekistan

⁹⁷Also at Northeastern University, Boston, Massachusetts, USA

⁹⁸Also at Imperial College, London, United Kingdom

⁹⁹Now at Yerevan Physics Institute, Yerevan, Armenia

¹⁰⁰Also at Universiteit Antwerpen, Antwerpen, Belgium